UNIVERSIDADE DE SÃO PAULO
INSTITUTO DE FÍSICA DE SÃO CARLOS

ANA GABRIELA VEIGA SEPULCHRO

Study of the lytic polysaccharide monooxygenases *Mt*LPMO9A for biotechnological applications

São Carlos
2021

ANA GABRIELA VEIGA SEPULCHRO

Study of the lytic polysaccharide monooxygenases *Mt*LPMO9A for biotechnological applications

Dissertation presented to the Graduate Program in Physics at the Instituto de Física de São Carlos, Universidade de São Paulo to obtain the degree of Master of Science.

Concentration area: Applied Physics
Option: Biomolecular Physics
Advisor: Prof. Dr. Igor Polikarpov

Original version

São Carlos
2021

Sepulchro, Ana Gabriela Veiga
Study of the lytic polysaccharide monooxygenases MtLPMO9A for biotechnological applications / Ana Gabriela Veiga Sepulchro; advisor Igor Polikarpov -- São Carlos 2021.
86 p.

Dissertation (Master's degree - Graduate Program in Biomolecular Physics) -- Instituto de Física de São Carlos, Universidade de São Paulo - Brasil , 2021.

1. Lytic polysaccharide monooxygenases. 2. Green-energy. 3. Enzyme characterization. 4. Light-activation. I. Polikarpov, Igor, advisor. II. Title.

FOLHA DE APROVAÇÃO

Ana Gabriela Veiga Sepulchro

Dissertação apresentada ao Instituto de Física de São Carlos da Universidade de São Paulo para obtenção do título de Mestra em Ciências. Área de Concentração: Física Biomolecular.

Aprovado(a) em: 23/06/2021

Comissão Julgadora

Dr(a). Igor Polikarpov

Instituição: (IFSC/USP)

Dr(a). Carlos Alberto Labate

Instituição: (ESALQ/USP)

Dr(a). Mario de Oliveira Neto

Instituição: (UNESP/Botucatu)

To my heavenly Father
and my earthly parents.

ACKNOWLEDGEMENTS

The Master's degree represents a stage in my path towards the construction of my future. One path that would be impossible to walk alone. And that is why I want to thank people who have been walked with me and have made this achievement possible.

First and foremost: to God, who gave me life. He guides and enlightens me wherever I walk. For from Him and through him and for Him are all things. To Him be the glory forever!

To my parents Carlos Pedro and Alessandra. What would I be without you? You are, without a doubt, my biggest supporters. I would never have gone anywhere if it weren't for your support. You have always encouraged me to fly, and knowing that I will always have a nest to return to makes me have the courage to fly far. I love you. This is all for you.

To Mari. My model since always. Thank you for being the personification of the whole family here in São Carlos during these years. And especially, thank you for had given life to the two most beautiful beings that I have ever met and that I love deeply: Loli and Maria.

To Ju. My other-half. Thank you for always supporting me even from a distance.

To Renan, for being my point of peace.

To my extended family, especially grandpa Mario and grandma Ana, aunt Deia, Tuco, Vivi, uncle Roger, Vini and Alexandre. For all the support.

To my Professor Igor Polikarpov, for the opportunity to be part of the Molecular Biotechnology Group, for your guidance, support and confidence. Thank you for teaching me how to be a scientist. Thank you for all the teachings and corrections that made me chase after knowledge.

To Vanessa, who has become much more than a co-advisor, has become a friend, a partner, a companion. My scientific mother. Words do not express my gratitude for you. Thank you for believing in me from the beginning. Thank you for the opportunity to collaborate together on so many cool works. Thank you for everything I learned from you.

To Lucas Danilo, who introduced me and my enzymes into the world of optics and became much more than a collaborator, became an example for me.

To Livinha, one of the best companies for laboratory problems and for heated discussions about series, film endings and new pop music. Thank you for the friendship and for introducing me to Tiquinho.

To all the other members of the group, especially Milena, Caio e Paula who made the research day by day lighter and more pleasant. To the technicians of the group: Maria Auxiliadora, Lívia, Josimar and João Possatto, for their promptness and assistance.

To the National Council for Scientific and Technological Development (CNPq), for financially supporting me and my research.

To the São Carlos Institute of Physics and the University of São Paulo, for excellence in infrastructure and teaching. For becoming my home for the last few years, always valuing and enabling the development of research.

And to all who collaborated directly or indirectly to carry out this work

my most sincere thanks!

ABSTRACT

SEPULCHRO, A. G. V. **Study of the lytic polysaccharide monooxygenases *Mt*LPMO9A for biotechnological applications.** 2021.86 p. Dissertation (Master in Science). Instituto de Física de São Carlos, Universidade de São Paulo, São Carlos 2021.

The growing demand for energy and the need to replace chemical technologies and non-renewable fuels in a sustainable and efficient way place the bioconversion of lignocellulosic biomass at the center of the current energy discussion. However, the high recalcitrance of this material makes its degradation a non-trivial task, even after undergoing physical-chemical pretreatments. The biotechnological solution applied to overcome this problem is the use of enzymes capable of acting synergistically in the efficient degradation of this biopolymers. In this context, lytic polysaccharide monooxygenases (LPMOs) oxygen and copper-dependent enzymes that demonstrate the ability to improve the performance of traditional hydrolytic enzymes have emerged. As it is an enzyme class with many peculiarities in relation to the others traditionally used in biomass bioconversion, the knowledge acquired in the last decade is disconnected, approaching several aspects of the enzyme in isolation. The present work aims to study the LPMO from *Thermothelomyces thermophilus* M77 (formerly *Myceliophthora thermophila*), connecting the main study points applied in LPMOs in a single enzyme. In the first part, a sequence and active site analysis was performed, as well as a biochemical characterization. The enzyme has a well-preserved active site among the LPMOs of the AA9 family, and has only the LPMO domain in its sequence. The enzyme has high thermal stability over a wide pH range (4 to 10), has a better performance on an amorphous cellulosic substrate and has ascorbic acid, as the preferred reducing agent among those tested. Regarding the co-substrate origin, *Mt*LPMO9A was able to use both H_2O_2 and O_2, however, for both cases, the need for high levels of reducing agent was observed. Another analysis revealed that the enzyme has a synergistic effect on cellulosic pulp degradation when combined with traditional cellulases cellobiohydrolase (Cel7A) and endoglucanase (Cel7B); leading to an increase of 83.17% and 84.00% in products generated in association with Cel7A and Cel7B respectively. The second part of the work was concerned with evaluating the use of *Mt*LPMO9A in photoactivated systems in the presence of photosensitizers. Starting with the commonly used chlorophyllin, this system made the enzyme much more efficient in the first reaction times, increasing the enzymatic activity in relation to the standard system. The investigation of the use of methylene blue as a photo-activator of *Mt*LPMO9A was also carried out, determining the ideal conditions of this system. Thus, it was possible to

generalize the LPMO/photosensitizer interaction, stating that the good performance of the latter in activating the enzyme is related to the mechanism by which it returns to its grounded state (Type I). The results obtained lead to an understanding of the mechanism of action of *Mt*LPMO9A, as well as pointing to its great potential in adding enzyme mixtures, increasing the efficiency of biomass conversion. In addition, by connecting the various aspects studied in LPMOs, such results help to build a solid and connected knowledge of this class of enzymes.

Keywords: Lytic polysaccharide monooxygenases. Green-energy. Enzyme characterization. Light-activation.

RESUMO

SEPULCHRO, A.G. V. **Estudo da monooxigenase lítica de polissacarídeo de *Mt*LPMO9A para aplicações biotecnológicas.** 2021. 86 p. Dissertação (Mestrado em Ciências). Instituto de Física de São Carlos, Universidade de São Paulo, São Carlos 2021.

A crescente demanda por energia e a necessidade de substituir tecnologias químicas e combustíveis não renováveis de forma sustentável e eficiente colocam a bioconversão da biomassa lignocelulósica no centro da discussão energética atual. No entanto, a alta recalcitrância desse material torna sua degradação uma tarefa não trivial, mesmo após submetida a pré-tratamentos físico-químicos. A solução biotecnológica aplicada para contornar este problema é a utilização de enzimas capazes de atuar sinergicamente na degradação eficiente deste biopolímeros. Nesse contexto, emergiram as monooxigenases líticas de polissacarídeos (LPMOs - do inglês: *lytic polysaccharide monooxygenases*), enzimas dependentes de oxigênio e cobre que demonstram capacidade de melhorar o desempenho de enzimas hidrolíticas tradicionais. Por se tratar de uma classe de enzima com muitas peculiaridades em relação às outras tradicionalmente empregadas na bioconversão de biomassa, os conhecimentos adquiridos na ultima década se mostram desconexos, abordando vários aspectos da enzima de forma isolada. O presente trabalho visa o estudo da LPMO de *Thermothelomyces thermophilus* M77 (anteriormente *Myceliophthora thermophila*), conectando os principais pontos de estudo aplicados em LPMOs em uma única enzima. Na primeira parte foi realizada uma análise de sequencia e de sítio ativo, bem como uma caracterização bioquímica. A enzima tem um sítio ativo bem conservado entre as LPMOs da família AA9, e possui apenas o domínio de LPMO na sua sequencia. A enzima tem alta estabilidade térmica em uma ampla faixa de pHs (4 a 10), possui melhor desempenho em um substrato celulósico amorfo e tem o ácido ascórbico, como o agente redutor preferencial dentre os testados. Em relação a origem de co-substrato, *Mt*LPMO9A se mostrou capaz de utilizar tanto H_2O_2 quanto O_2, entretanto, para ambos os casos era foi observado a necessidade de altos níveis de agente redutor. Outra análise revelou que a enzima tem um efeito sinérgico na degradação de polpa celulósica quando combinada com celulases tradicionais celobiohidrolase (Cel7A) e endoglucanase (Cel7B); levando um aumento de 83,17% e 84,00% nos produtos gerados na associação com Cel7A e Cel7B respectivamente. A segunda parte do trabalho se reteve em avaliar o uso da *Mt*LPMO9A em sistemas fotoativados na presença de fotossensibilizadores. Iniciando pela comumente usada clorofilina, esse sistema

fez com que a enzima fosse muito mais eficiente nos primeiros tempos de reação, aumentando a atividade enzimática em relação ao sistema padrão. Ainda foi realizada a investigação do uso do azul de metileno como foto-ativador da *Mt*LPMO9A determinando as condições ideais desse sistema. Dessa forma, foi possível generalizar a interação LPMO/ fotossensibilizador afirmando que o bom desempenho deste ultimo em ativar a enzima é relacionado ao mecanismo pelo qual ele retorna ao seu estado fundamental (Tipo I). Os resultados obtidos levam a uma compreensão do mecanismo de ação da *Mt*LPMO9A, bem como apontam para seu grande potencial em agregar misturas enzimáticas aumentando a eficiência da bioconversão da biomassa. Além disso, ao conectar os diversos aspectos estudados em LPMOs, tais resultados auxiliam na construção de um conhecimento sólido e conexo desta classe de enzimas.

Palavras-chave: Monooxigenases líticas de polissacarídeos. Energia-verde. Caracterização enzimática. Ativação por luz.

LIST OF FIGURES

LIST OF ABREVIATIONS, ACRONYMS AND SYMBOLS

•OH	Hydroxyl radicals
°C	Degrees Celsius
$^1O_2$	Singlet oxygen
AA	Auxiliary activities
ABF	Acetate/borate/sodium phosphate
AscA	Ascorbic acid
BSA	Bovine serum albumin
CAZy	Carbohydrate-active enzymes
CBM	Carbohydrate-binding module
CBP	Chitin-binding protein
CDD	Conserved domain database
Cel7A	*Trichoderma harzianum* cellobiohydrolase I
Cel7B	*Trichoderma harzianum* endoglucanase I
cm	Centimeter
DNS	Dinitrosalicylic acid
DS	Degree of synergism
DSMO	Dimethylsulfoxide
EDTA	Ethylenediaminetetraacetic acid
GallA	Gallic acid
GH	Glycoside hydrolase
H_2O_2	Hydrogen peroxide
HPAEC	High-performance anion exchange chromatography
I%	Increase in products release
IgG	Immunoglobulin G
kDa	Kilodaltons
L	Littre
L-cys	L-cysteine
LPMOs	Lytic polysaccharide monooxygenases
M	Molar
mg	Milligram
mL	Milliliter
mM	Mili molar
*Mt*LPMO9A	LPMO from *Thermothelomyces thermophilus* M77 (formerly *Myceliophthora thermophila*)
N_2	Molecular nitrogen
$NaHSO_3$	Sodium bisulfite
nm	Nanometer
O	Oxygen atom
O_2	Molecular oxygen
$O2^{\bullet -}$	Superoxide anion
PASC	Phosphoric acid swollen cellulose
PDB	Protein data bank

PDT	Photodynamic therapy
pH	Potential of hydrogen
pI	Isoelectric point
PyrA	Pyrogallic acid
QM/MM	Quantum mechanics/molecular mechanics
ROS	Reactive oxygen species
rpm	Rotations per minute
SAVES	Structural Analysis and Verification Server
Tm	Melting temperature
U	Enzyme unite
V-TiO_2	Vanadium-doped titanium dioxide
w/v	Weight/Volume
*x*g	G force
µL	Microliter
µM	Micromolar
µm	Micrometer

CONTENTS

PART I:

Enzymatic characterization of MtLPMO9A

Chapter 1

Introduction

Enzymatic biocatalysis of renewable lignocellulosic biomass is a key solution for circular economy and mitigation of the growing environmental impacts.[1-2] However, the high recalcitrance of plant biopolymers, makes their bioconversion a non-trivial task. Several biotechnological solutions, which can be applied to overcome this problem, are based on enzymes capable of acting synergistically in efficient degradation of carbohydrate polymers.[3-4]

In this context, lytic polysaccharide monooxygenases (LPMOs) have emerged. LPMOs are copper enzymes discovered about 10 years ago and since then, have been extensively investigated. Due to their ability to act synergistically with other cellulases, have become crucial components of the commercial enzymatic cocktails used in modern biorefineries. [5–7] The present work is a study on LPMO from *Thermothelomyces thermophilus* M77 (formerly *Myceliophthora thermophila*) (*Mt*LPMO9A).

In Part I, a sequence and phylogenetic analysis of the enzyme will be made, as well as a biochemical characterization, evaluation of the favorite co-substrate and synergism effect with traditional cellulases. But first, let's start by putting the main topics about this class of enzymes in context.

1.1 The discovery of lytic polysaccharide monooxygenases

It all started in the 1970's when Eriksson and collaborators demonstrated the presence of an oxidative enzyme in the culture of *Sporotrichum pulverulentum*. When conducting experiments with a concentrated culture in two different atmospheres (oxygen and nitrogen) and comparing these results with a mixture of endo and exo-glucanase in known concentrations, they determined the existence of enzymes that were responsible for double the amount of degraded cellulose and that had an oxidative character. To verify the generality of the existence of this type of enzyme in fungi considered extremely cellulolytic, this group of researchers further investigated three organisms - *Polyporus adustus*, *Myrothecium verrucaria*

and *Trichoderma viride* and noticed the repetition of this cellulose degradation improvement effect by an oxidative activity.[8] Even though the results obtained were innovative and fully in line to the old theory that cellulose needed to be activated first so that hydrolytic enzymes have access to fiber,[9] they have been unexplored for years.

A few years later, in the first decade of the present century, two discoveries *a priori* dissociated from the 1974 results were extremely important for the convergence of the oxidative class of enzymes. In 2005 Vaaje-Kolstad and collaborators described the non-catalytic enzyme chitin-binding protein CBP21 from *Serratia marcescens* belonging to the carbohydrate-binding module family 33 (CBM33).[10] Upon binding to chitin, CBP21 led to a disruption of the structure of the crystalline substrate and a dramatic increase in the efficiency of chitinases. The results of this study also showed that the effect of the CBP21 enzyme was not due to the formation of specific stoichiometric CBP21-chitinase complexes, but rather to a more general effect of CBP21 on substrate availability. Nonetheless, at that time it was not determined how CBP21 performed its interaction with chitin.

Later in 2010 Harris and Welner, together with collaborators, showed that certain proteins of the glycoside hydrolase family 61 (GH61) although lacking measurable hydrolytic activity alone, in the presence of divalent metal ions could significantly reduce the total protein load required to hydrolyze biomass lignocellulosic.[7] In addition to the need for these ions, their connection to two conserved histidines and the fact that this effect was only observed on non-pure cellulosic substrate, *i.e.*, in the presence of hemicellulose and lignin, were other discoveries in this study.

It was only later in 2010 that pieces would begin to come together. Vaaje-Kolstad showed, through experiments with CBP21, that the chitin-binding protein he had previously described was an enzyme that uses reducing power and molecular oxygen (O_2) to oxidatively cleave glycosidic bonds in chitin.[11] Besides, it was demonstrated in this study that the presence of a reducing agent such as ascorbic acid further increases the efficiency of these class of enzyme and that the removal of ions by ethylenediaminetetraacetic acid (EDTA) inhibited the activity that could be restored by adding divalent Mg^{2+} or Zn^{2+} ions that bond to the well-conserved histidine motif.

Over the next year, oxidative cellulose cleavage by both CBM33 [12] and GH61[13–16] has been demonstrated. It was then that the structural similarity and mode of action of the proteins from CBM33 and GH61 families pointed to the fact that they were members of a new class of enzymes - lytic polysaccharide monooxygenases (LPMOs). Hence, a need to reclassify these families into an appropriate carbohydrate-active enzymes (CAZy) category arose. As lignin is

invariably found together with polysaccharides in the plant cell wall and as the lignin fragments are likely to act in conjunction with LPMOs, it was decided to join the families of lignin-degrading enzymes to the LPMOs families and launch a new CAZy class that was called "auxiliary activities" to accommodate a variety of enzyme mechanisms and substrates.[17]

1.2 LPMOs families and substrate specificity

Currently, LPMOs are described in 7 different families according to their sequence similarities. These families are AA9, AA10, AA11, AA13, AA14, AA15 and AA16,[18] wherein LPMOs belonging to different families are not necessarily so different in terms of function. LPMOs can differ in terms of substrate specificity between families and even within a family (Figure 1).[19] The AA9 family (formerly GH61) has most of its members characterized with activity in cellulose, but it has some enzymes with activity in xylan, hemicellulose, xyloglucan, and lignocellulose. The AA10 family (formerly CBM33) has its members capable of oxidizing chitin and cellulose. The AA11, AA13, AA14 families, in its turn, present a substrate exclusivity, being active in chitin, starch, and xylan, respectively. The AA15 family has demonstrated activity in chitin and cellulose while AA16 only in cellulose.[18,20,21]

Although it is not yet possible to say with certainty what makes an LPMO capable of oxidizing one or another substrate, some factors are considered to be determinants.[20] Detailed structure and sequence comparisons showed that the substrate-binding surfaces of LPMOs with different substrate specificities have different amino acid compositions and topological features. These amino acids and topologies (*e.g.*, cavities near the catalytic Cu center), could hinder or favor the binding of certain substrates to LPMOs, thus being responsible for the diversity of interaction with substrates. The presence of carbohydrate-binding modules (CBMs) could also be a determining factor affecting the precise positioning of enzymes on the substrate surfaces.[20]

Albeit there are still few certainties on this subject, the fact is that the diversity of sequence and differences observed in the substrate specificity indicates that LPMOs can be involved in multiple different biological processes, which still need to be discovered, studied, and explored.

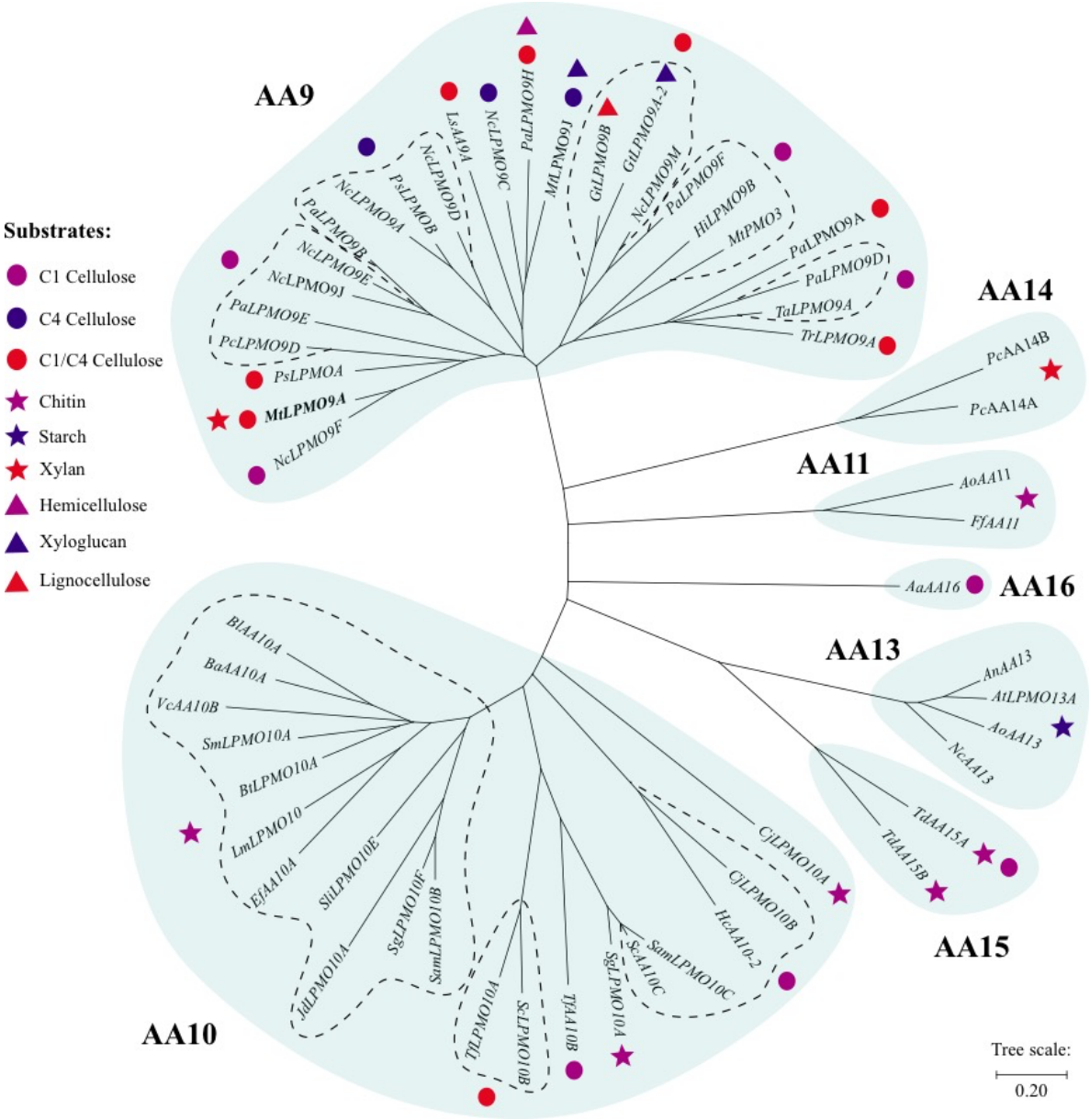

Figure1 - Phylogenetic tree of LPMOs. The tree was built with 56 sequences of LPMOs with substrate characterization available in the CAZy database.[18] The alignment was generated by Molecular Evolutionary Genetics Analysis software (MEGAX) [22] and phylogenetic analysis was performed at the same software using the neighbor-joining method.[23] The consensus tree was inferred using a bootstrap of 10,000 replicates. The tree was visualized and edited using MEGAX.
Source: By the author.

1.3 Oxidation mechanism and co-substrate preference

Unlike traditional hydrolytic enzymes that act on cellulose, LPMOs are oxidative enzymes, which cleave the substrate chain by oxidation on the C1 and/or C4 carbon of a sugar ring (Figure 2). When oxidation occurs at carbon C1, oligosaccharides are formed at its reducing end; the primary oxidation product is lactone which reaches equilibrium with its

hydrated form - an aldonic acid. When oxidation occurs in carbon C4 oligosaccharides are formed at the non-reducing end; a ketoaldose is produced as the primary oxidation product, being in equilibrium with the hydrated form 4-gemdiol-aldose.[19,24]

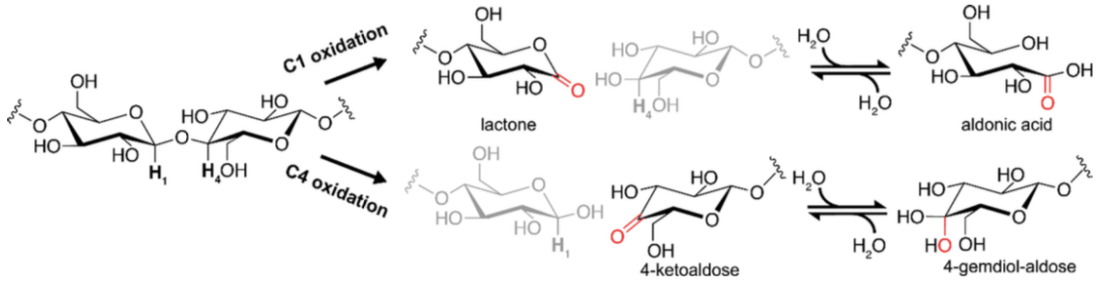

Figure 2 - Sugar ring oxidation patterns and the oxidized products generated during degradation catalyzed by LPMO.
Source: CHYLENSKI. *et al.* [19]

The oxygen activation to perform the cleavage of the glycosidic bond was first attributed to a monooxygenase action, where cleavage of the polysaccharide by the enzyme occurs in the presence of O_2 through the abstraction of an oxygen atom (O). In each catalytic monooxygenase cycle, LPMOs require the system to supply two free electrons and an oxygen molecule.[13,25] Besides to this monooxygenase mechanism, a study by Bissaro and collaborators in 2016 showed that LPMOs use a catalytic strategy based on harnessing and controlling the oxidative potential of hydrogen peroxide (H_2O_2) to cleave the substrate, thus having peroxygenase activity. [26] In this catalytic cycle, the external electron is only needed for the initial copper reduction, after which the cycle would be self-sustaining.

Despite the efforts of many studies, the molecular mechanism involving activation by both O_2 and H_2O_2 remained undetermined until very recently, when in 2019 Wang and colleagues, using hybrid analyzes of quantum mechanics/molecular mechanics (QM/MM) unveiled these mechanisms as well as their intermediates reactive, doing this in the presence of ascorbic acid and taking into account the presence of the substrate. [27]

Hence, this mechanism, which is currently the most accepted, says that LPMOs can have two pathways: O_2-dependent pathways and H_2O_2-dependent pathways (Figure 3). The O_2 dependent pathway has two distinct paths depending on whether protonation occurs in distal O (route I) or proximal O (route II). The latter case leads to the formation of a common intermediate with the H_2O_2-dependent pathway.[27,28]

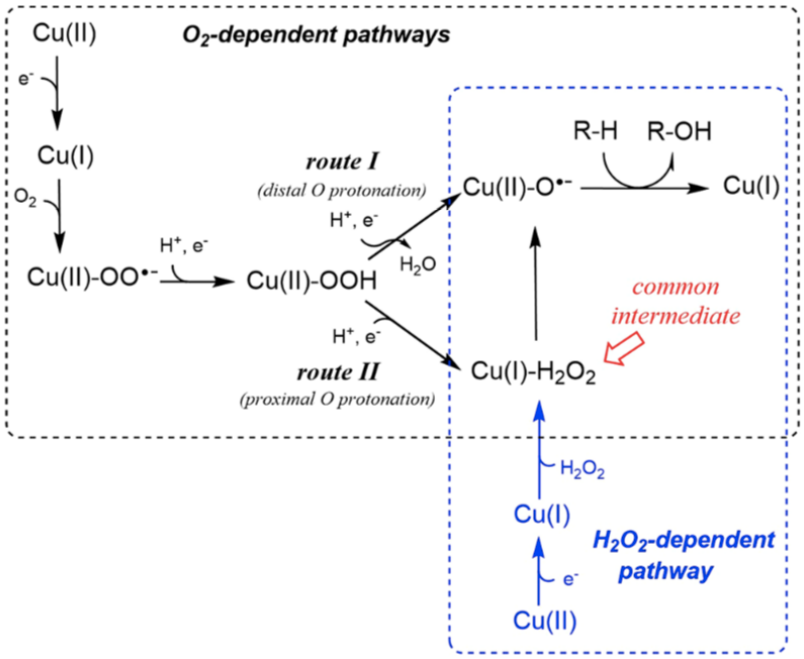

Figure 3 - Possible catalytic pathways: O_2 and H_2O_2-dependent activities of LPMOs.
Source: WANG; WALTON; ROVIRA.[27]

1.4 Uniqueness of the LPMO structure

Looking now from a structural view of LPMOs, the general structure makes them exclusively suitable to perform the catalysis in polysaccharides that are incorporated in the crystalline network, because unlike traditional glycoside hydrolases (GHs), which recognize the substrates in their enzymatic grooves or tunnels, LPMOs have an active site that coordinates the copper atom in the center of a flat surface.[24]

Although LPMOs between families and even within the same family may have, in general, a low sequence identity, they share very specific structural characteristics. LPMOs investigated structurally to date share the immunoglobulin G (IgG)-like β-sandwich fold and the vast majority of them have the histidine-brace motif.[14,29-30] Studies suggest that the aromatic side chains on the flat surface surrounding the active site bind to cellulose, similarly to CBMs.[31]

The Figure 4 taken from a recent review made by Tandrup and collaborators,[30] shows the general structure of the LPMOs from families AA9-11 and AA13-15. In the top line the Figure 4 shows histidine-brace, composed of an N-terminal His (methylated in fungal LPMOs) and an internal His for the equatorial Cu-coordination positions. In the bottom line, when showing the whole structure, the Figure 4 highlights the common IgG-like fold, with variation in surface topology (gray) depending on loop regions and helices.

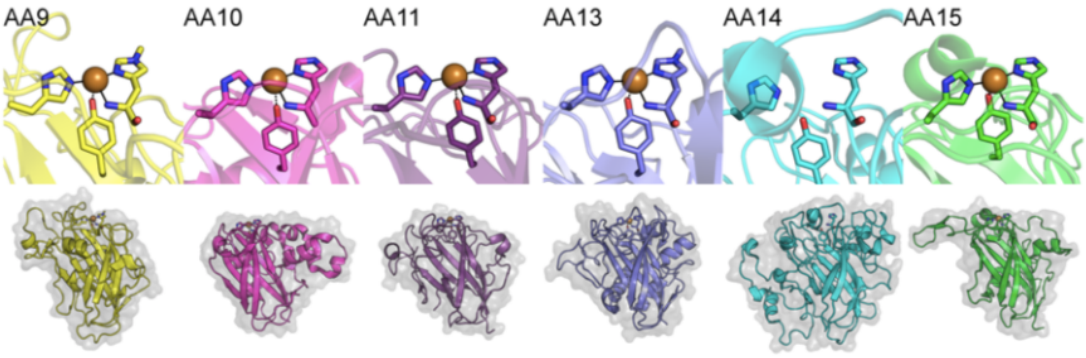

Figure 4 - Representative structures for LPMO families. PDB codes of the representing structures are: 5ACH (AA9, yellow), 5OPF (AA10, magenta), 4MAI (AA11, purple), 4OPB (AA13, dark blue), 5NO7 (AA14, cyan) and 5MSZ (AA15, green).
Source: TANDRUP *et al.*[30]

It is worth mentioning at this point that there is an exception regarding histidine-brace. Some protein sequences belonging to the AA9 LPMO family, found almost entirely in the phylogenetic fungi class *Agaricomycetes*, have a natural substitution of His for Arg at the N-terminus (Arg-AA9) (Figure 5).[32] To date, no function has been demonstrated for any Arg-AA9, although bioinformatics analyzes suggest the existence of a putative biological function for Arg-AA9s related to the degradation of lignocellulosic biomass.[32-33]

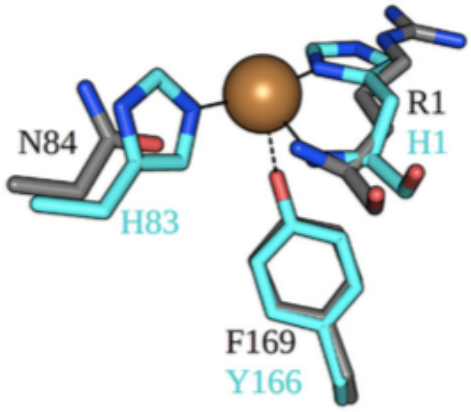

Figure 5 - Active site residues of the structurally closest homolog *Nc*AA9C (cyan, PDB 4D7U) superimposed onto the equivalent residues of *Ls*AA9B, a Arg-AA9 protein.
Source: FRANDSEN *et al.* [33]

1.5 The biological context of LPMOs

Once clarify the main characteristics of LPMOs, let's delve into the roles of this enzymes. In nature, LPMOs are found in several types of organisms; families AA9, AA11, AA13, AA14 and AA16, originate mainly from eukaryota. The AA10 family, are from bacteria, eukaryota, viruses or archea. And the AA15s family are from eukaryota (including

insect) or viruses.[20] However, the biological role of the multiplicity of genomes and species of origins is not yet fully understood. Many studies have been carried out to unveil the relevance of these enzymes in nature and it is currently known that the AA9, AA15 and AA16 families are of particular importance from the point of view of the plant-pathogen and plant-insect interaction (Figure 6).[34]

Starting with the AA9 family, its members are found exclusively in fungi and have the main catalytic activity against cellulose. Fungi are among the main causative agents of plant diseases and almost 90% of all known lignocellulose-degrading fungi contain genes encoding AA9 LPMOs.[35] AA9 enzymes are, therefore, the largest family of LPMOs [36] that can serve as virulence factors in pathogenicity, allowing pathogens to infect successfully. Another family that deserves mention in this theme is the recent discovery AA16, which has its enzymes with origins in fungi and oomycetes with pathogenic and saprophytic lifestyles. The major fungal pathogens known to carry AA9 genes also contain genes encoding AA16 in their genomes in both *Ascomycota* and *Basidiomycota*. And therefore, the interaction of these enzymes with pathogenic activity is imminent.[34]

Moving now to the AA15 family, recently identified in a primitive insect (*Thermobia domestica*),[37-38] enzymes from this family have activity characterized in both cellulose and chitin. The hypothesis about these enzymes is that they were originally recruited to assist the process of remodeling the chitin-rich exoskeleton during metamorphosis, but that later acquired the ability to digest cellulose. The ability to digest recalcitrant plant cell walls is one of the main reasons for the success of herbivorous insects in becoming notorious pests in various agricultural plants. The occurrence of genes encoding AA15 in the genome of various agricultural pests reinforces the view that, endogenous enzymes fully capable of degrading the cell wall on their own are a possibility.[34]

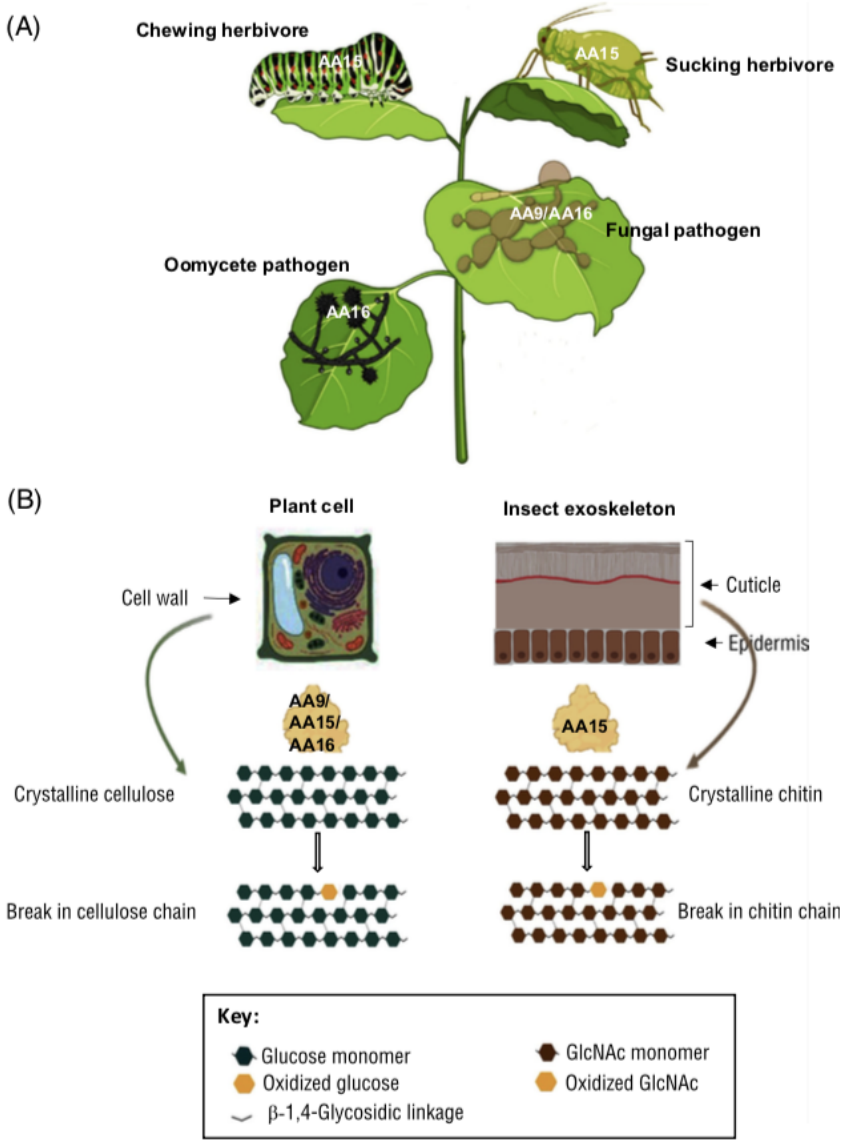

Figure 6 - LPMOs in plant–biotic interactions. (A) LPMO families AA9, AA15, and AA16 are of particular relevance in plant–pathogen and insect interactions. (B) The major polysaccharide component in plant cell walls is cellulose and chitin in insect exoskeletons. Both are recalcitrant to degradation because of their crystalline nature.
Source: JAGADEESWARAN; VEALE; MORT.[34]

In addition to these interactions with plants, there is also a pathogenic interaction associated with the LPMOs of the AA10 family. This family acts on chitin or cellulose occurring mainly in bacteria and interestingly, several human pathogenic bacteria contain genes that code AA10 LPMOs that are identified as virulence factors, which help in the infection and evasion of immune response of the host.[39]

1.6 Biotechnological applications of LPMOs in biomass depolymerization

It is not because of its pathogenicity that LPMOs have attracted much interest, but because of the biotechnological application they can serve. The growing global demand for energy combined with concerns about problems arising from the use of fossil fuels raises more and more the use of bioenergy as an energy alternative.[40] One of the current challenges concerning obtaining ethanol and then consolidating this renewable fuel in the face of fossil fuels is to increase its production without increasing the area for planting raw materials. This is applicable through the energy use of biomass,[41] lignocellulosic plant material consisting of three types of polymers: cellulose, hemicellulose, and lignin.[42]

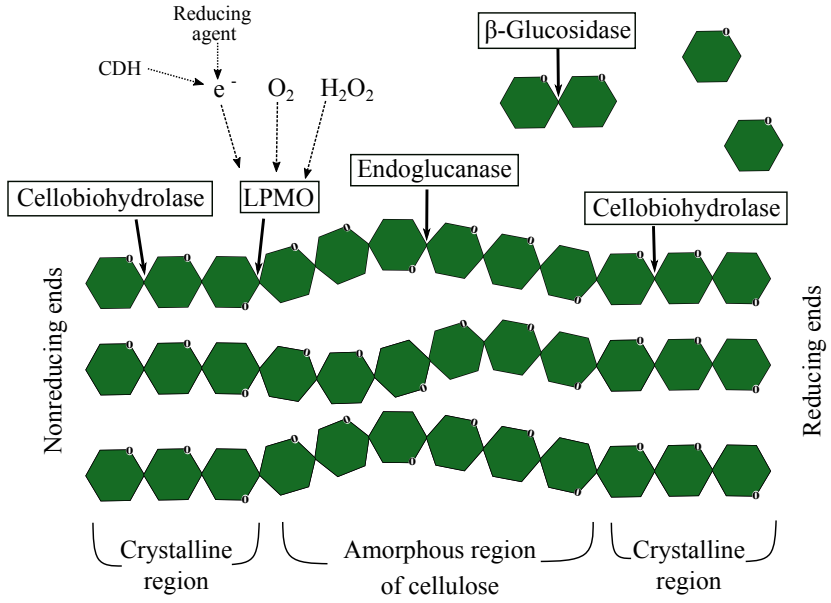

Figure 7 - Schematic representation of the enzymatic degradation of cellulose.
Source: PELLEGRINI; SEPULCHRO; POLIKARPOV.[43]

Since the enzymatic hydrolysis of biomass biopolymers is one of the costliest technological steps in the valorization of second-generation ethanol, it is necessary the use of enzymes that are capable of making this process efficient and at the same time more economically viable and sustainable (Figure 7).[4] In this context, LPMOs appear as a possible alternative. These enzymes can improve the activity of GHs, increasing the yield of enzymatic hydrolysis of the polysaccharides present in the biomass.[44] Hence, showing as a promise to boost the capacity of enzymatic cocktails, ensuring improvements in the general process of obtaining second-generation ethanol.[24]

Chapter 2

Objectives

2.1 Overall objectives

In view of the above, the study of LPMOs that make the biomass depolymerization process more economically viable and sustainable is essential. For this reason, the present work focused on the study of an LPMO from *Thermothelomyces thermophilus* M77 (formerly *Myceliophthora thermophila*) (*Mt*LPMO9A), aiming to connect all the main points of study in a single enzyme and thus makes it a model for high-performance LPMOs in biotechnological processes.

The overall Part I objective consists of the molecular and biochemical characterization of this enzyme, analyzing its mode of action, preference of substrate, reducing agent and co-substrate, as well as its interaction with traditional cellulases.

2.2 Specific objectives

- Sequence and phylogenetic analysis;
- Analysis of the *Mt*LPMO9A cupper active site via homology model;
- *Mt*LPMO9A heterologous expression and purification;
- Characterization in terms of ideal substrate and reducing agent;
- Determination of *Mt*LPMO9A stability conditions by Thermofluor assay;
- Determination of the preferred *Mt*LPMO9A co-substrate;
- Determination of synergism with traditional cellulases from glycoside hydrolase family 7 (GH7).

Chapter 3

Material and methods

3.1 Sequence and phylogenetic analysis

The amino acid sequence of *Mt*LPMO9A from *Thermothelomyces thermophilus* M77 (formerly *Myceliophthora thermophila*) (GeneBank: MYCTH_85556, UniProt: KP901251) was submitted to CDD: NCBI's conserved domain database, for an initial analysis.[45] Then, the presence of post-translational modifications (signal peptide and glycosylation) was evaluated. For the signal peptide, the web software SignalIP3.0 was used.[46] To assess the presence of glycosylation, the NetNGlyc web software was used (http://www.cbs.dtu.dk/services/NetNGlyc/) for N-linked glycosylation and NetOGlyc (http://www.cbs.dtu.dk/services/NetOGlyc/) for O-linked glycosylation.[47] The sequence of the mature protein was subjected to analysis by ProtParam tool from ExPASy (http://web.expasy.org/protparam/).

Then, the *Mt*LPMO9A mature sequence was submitted to BLAST (https://blast.ncbi.nlm.nih.gov/Blast.cgi?PAGE=Proteins). Twenty-four sequences were selected and used for constructing the phylogenetic tree. Phylogenetic analysis was performed with the sequence alignment generated with Evolutionary Genetics Analysis software (MEGAX)[22] using the ClustalW algorithm.[48] The alignment file was used in the same software and the neighbor-joining method [23] was used to generated a consensus tree inferred using a bootstrap of 10,000 replicates. The tree was visualized and edited using MEGAX.

3.2 Structure homology modeling

Based on the mature amino acid sequence from *Mt*LPMO9A, a structure model was built using the web-based software SWISS-MODEL.[49] For that, it was used the crystal structure of the zinc-bounded LPMO9E from *Thielavia terrestris* as template (PDB:3EII)[7] and the structural figures were generated using the PyMOL Molecular Graphics System (Version 1.5.0.4 Schrödinger, LLC, New York, NY, USA). The quality of the generated model was evaluated by ERRAT[50] via Structural Analysis and Verification Server (SAVES) web tool.

3.3 Enzymes production and purification

The coding sequence of *Mt*LPMO9A (MYCTH_85556, UniProt: KP901251) was amplified from genomic DNA, cloned, and the expression plasmid was transformed into *Aspergilus nidulans A773* by Prof. Dr. Fernando Segato as previously described [51–54] and recombinants strains were kindly provided to Molecular Biotechnology Group.

The recombinant expression of *Mt*LPMO9A was conducted in a static liquid medium. First, *A.nidulans Mt*LPMO9A recombinant strain was activated in minimal solid medium containing 100 mg/L of pyridoxine, 50 mg/L of nitrate salts (120 g/L of $NaNO_3$, 10.4 g/L of KCl, 10.4 g/L of $MgSO_4$ and 30.4 g/L KH_2PO_4), 1 mL/L of trace element (22 g/L of $ZnSO_4$, 11 g/L of H_3BO_3, 5 g/L $MnCl_2$, 1.6 g/L of $CaCl_2.5H_2O$, 1.6 g/L of $CuSO_4.5H_2O$, 5 g/L of $FeSO_4.7H_2O$, 1.1 g/L of $NaMoO_4.4H_2O$ and 50 g/L Na-EDTA), 10 g/L of glucose and 19 g/L of agar at pH 6.5.

After 48 h at 37 °C the resulting spores (approximately 10^7-10^8 spores/mL) were transferred to 0.5 L induction medium composed of minimum medium supplemented with 50 g/L maltose. The heterologous expression was conducted for 40 hours at 37 °C, then mycelial mat was removed, and the culture medium filtered using Miracloth membranes (Merck KGaA Darmstadt, DE).

The filtrate was collected and centrifuged for 20 minutes, 20,000 *x*g at 4 °C. Then the medium was subjected to a second filtration on Miracloth membranes (Merck KGaA Darmstadt, DE) before the concentration step using the Hollow Fiber system (5 kDa cutoff) (GE Healthcare, Chicago, USA) to reduce volume. The protein sample was further purified by 70% (w/v) ammonium sulfate precipitation under constant agitation at 10 °C for 16 hours. The sample was centrifuged for 30 minutes, 20,000 *x*g at 4°C and the pellet resuspended in 10 mL of 20 mM Tris-HCl buffer, pH 8.0 and another centrifugation step was performed under the same conditions. The supernatant was subjected to a first purification step in a 5 mL Q-Sepharose™ Fast Flow column, where the *Mt*LPMO9A was collected at flow-thought. Then, a hydrophobic interaction chromatography in the HiLoad Phenyl Sepharose 26/10 column (GE Healthcare, Chicago, USA) was performed. Elution was performed with 20 mM Tris-HCl, pH 8.0 and 20 mM Tris-HCl buffers added to 1M $(NH_4)_2SO_4$, pH 8.

In the last molecular exclusion chromatography step, *Mt*LPMOA9 was copper-saturated with Cu(II)SO_4 with a three-fold molar excess and then applied into a HiLoad 16/600 Superdex 75 pg column (GE Healthcare, Chicago, USA) coupled to an Äkta Purifier

10 system. The protein was eluted using an isocratic gradient of 20 mM Tris-HCl buffer at pH 8 and 150 mM NaCl.

For synergism analysis, *Trichoderma harzianum* endoglucanase I (Cel7B) and *Trichoderma harzianum* cellobiohydrolase I (Cel7A) were expressed and purified as previously described.[55-56]

3.4 Thermal stability analysis by Thermofluor assay

Thermofluor assay was used to determine the effects of pH on the structural stability of *Mt*LPMO9A. The measurements were performed in a pH range from 2 to 10 using the acetate/borate/sodium phosphate buffer (ABF) from a 100 mM stock solution. 5μL of the enzyme at 1.5 mg/mL concentration (standard test condition) was used with a 5,000x concentrate SYPRO Orange dye (Invitrogen; California, USA) diluted in dimethylsulfoxide (DSMO). Samples were incubated in an iCycler iQ Real-Time PCR Detection System (Bio-Rad, USA) within a temperature range from 25 to 90 °C with stepwise increments of 1 °C per minute and 10-s hold step. To determine the melting temperatures (Tm), fluorescence intensity was monitored with excitation at 490 nm and emission at 530 nm.

3.5 High-performance anion exchange chromatography (HPAEC) analysis

The analysis of LPMO reaction products was performed by a High-performance anion exchange chromatography (HPAEC) system (ICS-5000, Dionex, Sunnyvale, USA), equipped with a CarboPAC1 analytical column 250 mm × 2 mm (Dionex, Sunnyvale, USA). For sample elution, two solutions were used: a 100 mM NaOH (solution A) and a 500 mM sodium acetate plus 100 mM NaOH (solution B). The flow rate was set at 0.3 mL/min at 30 °C. The injection volume was 1 μL and the elution was performed using the steps procedures using the following steps: isocratic separation (10 min, 100% A), gradient separation (20 min, 10-100% B), column wash (8 min, 100% B), equilibration (5 min, 100% A). Chromatograms were recorded and analyzed using Chromeleon 7.0 software.

Pure cello-oligosaccharides (all from Megazymes, Wicklow, Ireland) and oxidized cello-oligosaccharides (prepared as described by Keller *et al*. [57]), were used as the standards for identification and quantification of generated products. To quantify the generated products, 120 μL of the soluble product was mixed with 0.1 μM of *Trichoderma harzianum* endoglucanase I (Cel7B) [55] in 20 mM citrate buffer pH 5 followed by an overnight incubation at 50 ºC.

3.6 Substrate specificity and electron donor preference

The standard basis for enzymatic reaction was 1μM of *Mt*LPMO9A, mixed with 0.3% (w/v) of specified substrate and 1 mM of specified reducing agent, in 20 mM of sodium citrate buffer pH 5.0. The reactions were conducted for 16 hours at 50 ºC and 1000 rpm.

To evaluated the substrate specificity ascorbic acid (AscA) was used as electron donor and phosphoric acid swollen cellulose (PASC) prepared from Avicel PH-101 (Sigma-Aldrich, St. Louis, USA) as described by Wood,[58] Avicel (Sigma-Aldrich, St. Louis, USA), bacterial cellulose (lab-made) and filter paper from Whatman (Maidstone, United Kingdom) were tested. The evaluation of the ideal electron donor was performed using PASC as substrate and ascorbic acid (AscA), L-cysteine (L-cys), pyrogallic acid (PyrA) and gallic acid (GallA) (all from Sigma-Aldrich, St. Louis, USA) were tested from a 100 mM stock solution in water.

After reaction time, samples were boiled at 95 °C for 5 minutes, centrifuged at 9,600 *x*g for 10 minutes at 4 °C, separated from the insoluble substrate by filtration in a 0.22 μm filter and then analyzed by HPAEC.

3.7 LPMO activation in the presence of O_2 and/or H_2O_2

3.7.1 Analysis for the optimum H_2O_2 activation condition

To determine the use of H_2O_2 by *Mt*LPMO9A as a co-substrate, we first evaluated the enzyme activation by the fixed concentration of H_2O_2 (50 μM) and varying the concentrations of AscA (20 μM, 100 μM, 500 μM and 1 mM) in 4- hour reactions. After determining the best ascorbic acid condition, this condition was fixed and the H_2O_2 concentration was varied as 50 μM, 100 μM, 250 μM and 500 μM, at 4-hour reaction times. This evaluation was performed using PASC 0.3 % (w/v) at in 20 mM of sodium citrate buffer pH 5.0, at 50 ºC and 1000 rpm.

3.7.2 Comparison of activation by H_2O_2 X O_2 over time

The optimized condition for PASC was evaluated over time, in presence and absence of H_2O_2. The evaluated time were 5 min, 15 min, 30 min, 1 hour, 2 hours, 4 hours and 6 hours. After each reaction time, the generated products were quantified and the apparent H_2O_2 was mesured.

To mesure the apparent H_2O_2 the method was addapeted from previosly reported protocol.[59] 50 µL were sampled and filtrated at the evalueted intervals of time and mixed with 50 µM Amplex Red reagent and 7.1 U mL^{-1} horseradish peroxidase (both from Sigma-Aldrich) in 100 mM of sodium phosphate buffer pH 6.0 in a 100 µL final volume. The reaction was incubated at 30 ºC in a spectrophotometer and measured at 563 nm.

3.7.3 Evaluation of product generated under different conditions of oxygen sources

Finally, the role of O_2 and H_2O_2 as oxygen source was evaluated under molecular nitrogen (N_2) atmosphere, using PASC substrate. To confirm that the enzymatic reactions were performed under low oxygen tension, the O_2 pressure was measured using the NeoFox optical oxygen sensor (OceanOptics). When present, H_2O_2 was added in a 50 µM final concentration. These reactions were performed for 30 minutes.

3.8 Evaluation of *Mt*LPMO9A synergistic action with GH7 cellulases

To evaluate the synergy of *Mt*LPMO9A with GH7 cellulases from *Trichoderma harzianum*, an endoglucanase (Cel7B)[55] and a cellobiohydrolase (Cel7A)[56] were used. The activity of these enzymes was evaluated using Eucaliptus cellulose pulp (Aracruz Celulose, Aracruz, ES, Brazil) in a 5% (w/v) reaction. The amount of enzyme in each reaction was 1 mg of total enzyme per gram of substrate. The generated products were determined by the dinitrosalicylic acid (DNS) method,[60] using a glucose calibration curve. Reactions occurred in 20 mM sodium phosphate buffer at pH 6.0, at 50 ºC, 1000 rpm, and were carried out in triplicates. Controls in the absence of enzymes were also evaluated. The evaluated times were: 1, 2, 4, 6, and 8 hours.

Reactions consisted of: i) enzymes alone, ii) Cel7B or Cel7A in the presence of *Mt*LPMO9A - in a proportion of 50% of each enzyme; iii) 50% of enzyme plus 50% of bovine serum albumin (BSA). The degree of synergism (DS) and the increase in products release (I%) were calculated as follows:

$$DS = \frac{A_{(cellulase + MtLPMO9A)}}{A_{(cellulase + BSA)} + A_{(MtLPMO9A+BSA)}}$$

$$I(\%) = \frac{A_{(cellulase + MtLPMO9A)} - (A_{(cellulase + BSA)} + A_{(MtLPMO9A+BSA)})}{A_{(cellulase + MtLPMO9A)}} X\ 100$$

Chapter 4

Results and discussion

4.1 Sequence analysis and enzyme production and purification

The primitive *Mt*LPMO9A sequence has 225 amino acids and according to the CDD, it has only one LPMO AA9 domain identified between amino acids 18 and 223. A more detailed analysis has shown that the first 17 amino acids in this sequence correspond to signal peptide and that this enzyme has no sites for potential N-linked glycosylation and has only one site for potential O-linked glycosylation (Ser-187) (Figure 8a).

The 208 amino acid sequence of the mature protein was submitted to ProtParam resulting in a theoretical mass of 22.75 kDa, theoretical isoelectric point (pI) of 6.6, and an extinction coefficient of 44140 M^{-1} cm^{-1}, at 280 nm. *Thermothelomyces thermophilus M77* LPMO was then successfully expressed in *Aspergilus nidulans* A773, and the purification steps employed resulted in the pure protein close to 25 kDa in the SDS-PAGE gel, as can be seen in the Figure 8b.

Figure 8 - Sequence analysis and enzyme purification. a) *Mt*LPMO9A signal peptide in a cyan box, catalytic domain in a purple box, predicted O-linked glycosylation marked in a blue circle. b) SDS-PAGE gel of *Mt*LPMO9A after all purifications step. L represents the ladder of molecular mass and 1 is the protein sample.
Source: By the author.

4.2 Phylogenetic analysis

To gain insights into evolutionary differences between *Mt*LPMO9A from the homologous enzymes, a phylogenetic tree was built with the sequences that had regioselectivity available at CAZy database;[18] the generated tree can be seen in Figure 9. It is clear that enzymes with the same regioselectivity tend to stick to the same branch of the tree. Interestingly, the branch of the tree on which *Mt*LPMO9A is found in the branch does not have a clear separation of regioselectivity. The enzyme is close to enzymes with oxidation pattern at the C1 carbon of cellulose C1 carbon, as well as with enzymes with oxidation pattern at the C1- and C4- carbon of cellulose. Indeed, previous characterizations describe this enzyme with C1/C4 oxidizing regioselectivity,[61-62] but its proximity to C1 oxidizing enzymes may be indicative of a pattern preference.

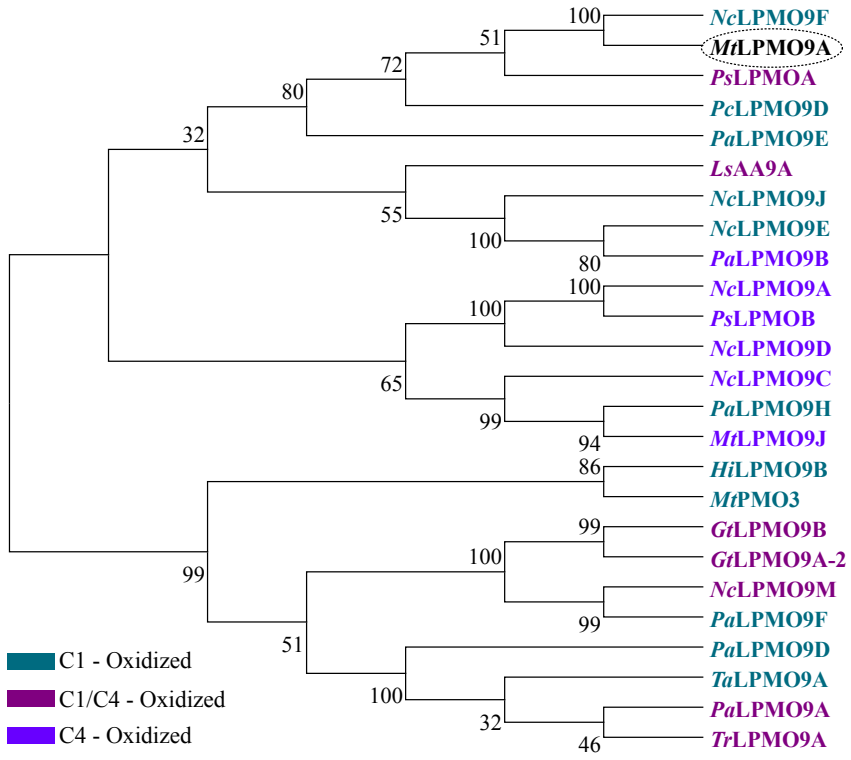

Figure 9 – Phylogenetic tree analysis. Enzymes are marked by colors according to their regioselectivity available CAZy database.[18] Enzymes with oxidation C1 are found in green, oxidation C1/C4 in wine and oxidation C4 in light purple. The study enzyme of the present work (*Mt*LPMO9A) is outlined in black in a dotted circle.
Source: By the author.

4.3 *Mt*LPMO9A cupper active

The analysis of the active copper site of *Mt*LPMO9A was performed using the homology model built from the crystal structure of the zinc-bounded LPMO9E from *Thielavia terrestris* (PDB: 3EII),[7] which has a sequence identity of 76.92% with *Mt*LPMO9A. The generated model was evaluated by ERRAT [50] via Structural Analysis and Verification Server (SAVES) web tool; the overall quality factor provided by ERRAT was 87,245%.

The general structure of the *Mt*LPMO9A shows the immunoglobulin G-like β-sandwich fold (Figure 10a) and the analysis of the copper site showed that the ion is coordinated by four amino acids (Figure 10b), being two histidines (His-1 and His-68) and two tyrosine (Try -67 and Try-153), on a flat surface. In addition to the histidines characteristic of the histidine-brace of LPMOs, the other pair of aromatic amino acids that are part of the copper-binding site highlights the fact that suggests that the aromatic side chains on the flat surface surrounding the active site bind to cellulose, similarly to CBMs.[31] It may be an indication that such structure favors *Mt*LPMO9A to bind to cellulosic substrates.

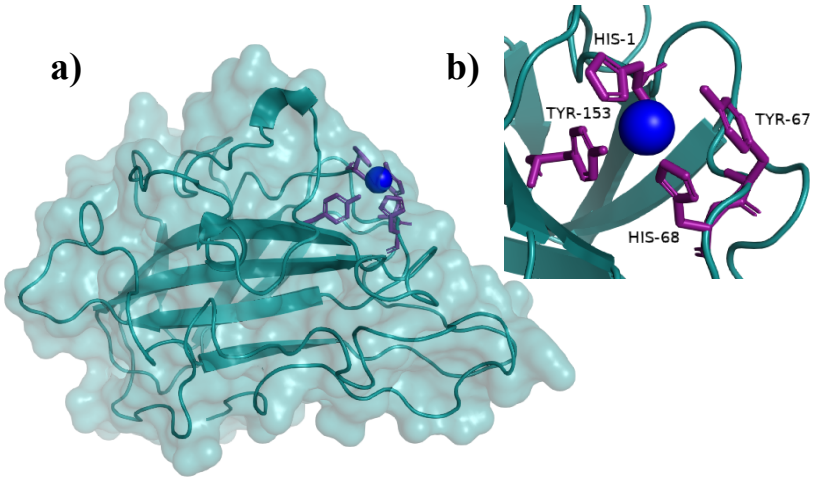

Figure 10 – Overall structure of *Mt*LPMO9A generated via homology modeling. a) Surface topology of *Mt*LPMO9A highlighting the IgG-like fold. b) Cupper active site.
Source: By the author.

4.4 Thermal stability analysis by Thermofluor assay

The differential scanning fluorimetry experiments were carried out to monitor the thermal stability of the protein, allowing the identification of the best pHs for maintaining the stability of the *Mt*LPMO9A tertiary structure, as a function of temperature. The result can be seen in Figure 11. For the most acidic pHs analyzed, 2 and 3, it can be seen that the

fluorescence spectrum has its maximum presented at lower temperatures (Figure 11a). Representing that at these pHs the protein is less stable and unfolds at these temperatures thus exposing the probe.

However, *Mt*LPMO9A showed high thermal stability at pHs from 4 to 10. From pH 5, the protein shows a small variation, showing itself to be equally stable at pHs as alkalinity increases with an average denaturation temperature of 78.5 °C ± 2 °C in this range (Figure 11a and b).

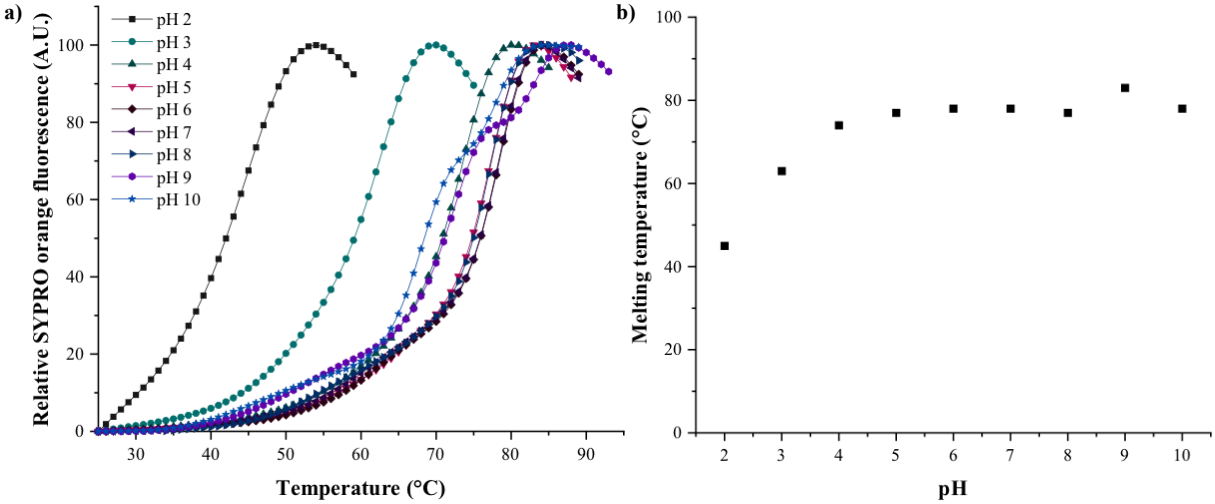

Figure 11 – Thermofluor assay analysis. a) Relative SYPRO orange fluorescence within the range of pHs 2 to 10. b) Melting temperature of *Mt*LPMO9A in the same pH range.
Source: By the author.

4.5 Substrate specificity and electron donor preference

*Mt*LPMO9A activity was evaluated using PASC, Avicel, filter paper, and bacterial cellulose as cellulosic substrates in 16 hours reactions. Under tested conditions, *Mt*LPMO9A activity was highest against PASC (Figure 12a). This selectivity may be due to the higher accessibility of the latter substrate which facilitates its oxidative cleavage by the enzyme. *Mt*LPMO9A generated both C1- and C4- oxidized cellopyranose residues. However, the enzyme showed a clear preference for oxidation at the C1 position over the C4 and C1/C4 positions. This fact is in line with the evolutionary analysis performed shown in Figure 9.

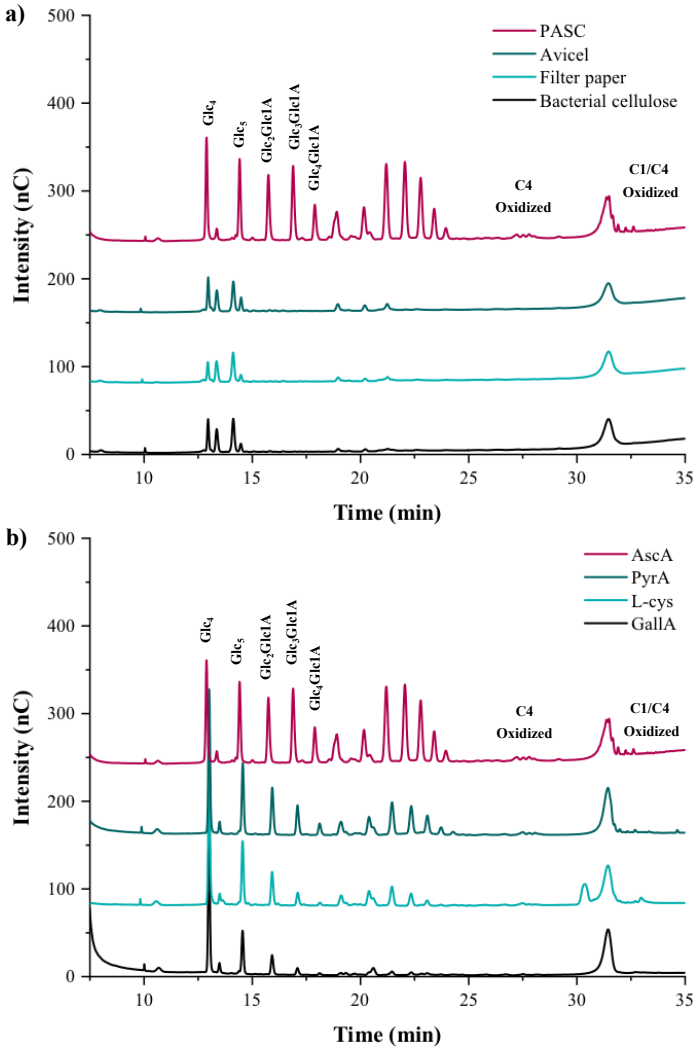

Figure 12 – *Mt*LPMO9A specificity for substrate and electron donor. a) *Mt*LPMO9A (1 μM) activity in different cellulosic substrate. *Mt*LPMO9A has a clear preference for PASC, a more amorphous and less recalcitrant substrate. b) Evaluation of the difference in enzymatic activation of different reducing agents, using PASC as a substrate. The highlighted non-oxidized oligosaccharides are Glc4 (cellotetraose) and Glc5 (cellopentaose). C1-oxidized oligosaccharides are GlcGlc1A (cellobionic acid), Glc2Glc1A (cellotrionic acid), Glc3Glc1A (cellotetraonic acid) and Glc4Glc1A (cellopentaonic acid).
Source: By the author.

The selectivity of *Mt*LPMO9A for different reducing agents was also evaluated in a 16 hours reaction using ascorbic acid, pyrogallic acid, gallic acid, and L-cysteine (Figure 12b). These chemical electron donors can be classified into three distinct groups based on the structural similarities of their functional groups.[61] Gallic and pyrogallic acid comprise a group of compounds with a 1,2,3-benzenetriol moiety. L-cysteine belongs to a group of sulfur-containing compounds and ascorbic acid comprises a group of reducing agents that do not have neither a phenolic ring nor a sulfur atom.

Among the analyzed compounds, gallic acid promoted weakest activation of *Mt*LPMO9A. Ascorbic acid was responsible for the strongest LPMO activation, followed by

pyrogallic acid and by L-cysteine (Figure 12b). Ascorbic acid is used extensively in LPMO studies,[11,13,63–66] and although the reason why it usually performs better in LPMO reduction is not completely clear,[67] molecular dynamic simulations using the quantum mechanics/molecular mechanics (QM/MM) method have already demonstrated that ascorbate is rapidly reducing LPMO-Cu(II) following a thermodynamically favorable process.[27-28] Furthermore, the same simulations indicated that the electron transfer in this system is mediated by water molecules, thus potentially revealing requirement of ascorbate to bind the LPMO to accomplish copper reduction.[27-28]

4.6 LPMO activation in the presence of O_2 and/or H_2O_2

The LPMO mechanism remains a subject of discussion, even though recent studies have shown that both catalytic pathways (monooxigenases and peroxygenase) are possible.[27-28] However, it still remains unclear what determines the preferential catalytic pathway for a particular LPMO.

4.6.1 Analysis for the optimum H_2O_2 activation condition

To analyze the co-substrate preferences of *Mt*LPMO9A, it was first fixed a H_2O_2 concentration to assess the optimum concentration of the ascorbic acid required for the catalytic process to occur.

In the LPMO peroxygenase pathway, the reducing agent could only be necessary for the initial reduction of LPMO-Cu (II) to LPMO-Cu (I) (known as priming), initiating an electronically self-sustaining oxidation process. The experimental results in PASC demonstrated that the quantity of products generated by *Mt*LPMO9A were increasing with the increasing concentrations of ascorbic acid until 500 μM, reaching a plateau (Figure 13a).

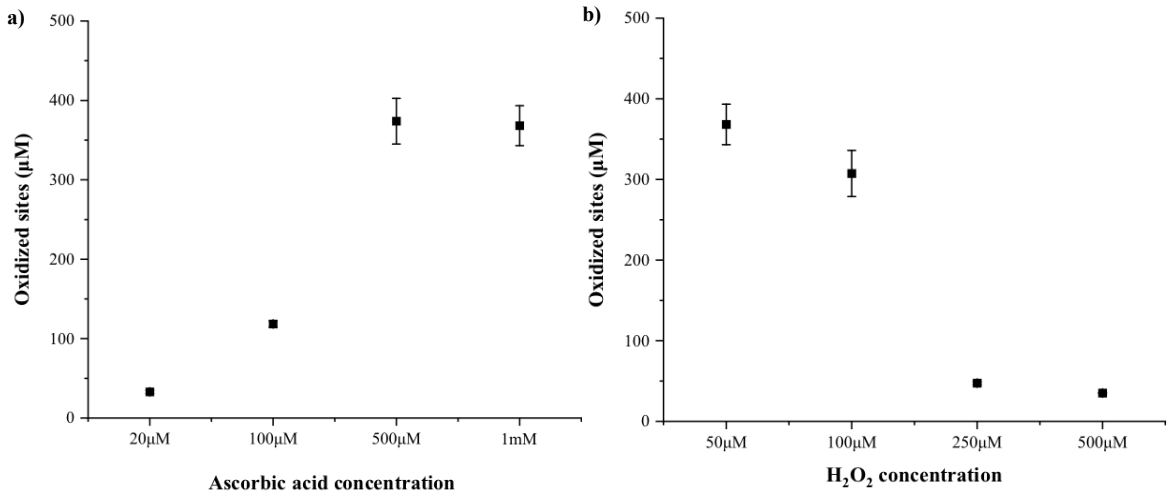

Figure 13 – Evaluation of the optimum conditions for peroxygenase reaction of *Mt*LPMO9A (1 µM) on PASC. a) reaction was performed with a fixed H_2O_2 concentration of 50 µM, varying the amount of ascorbic acid from 20 µM to 1mM; b) Ascorbic acid concentration was fixed at 1mM and the amount of H_2O_2 was varied from 50 µM to 500 µM.
Source: By the author.

Then, the ascorbic acid concentration was set in 1 mM and the H_2O_2 concentration was varied to study the influence of different concentrations of co-substrate in the reaction medium on the LPMO activity (Figure 13b). It was observed that products accumulation showing a decrease in the product released for concentration higher than 50 µM of H_2O_2, until almost total inactivation of the enzyme by 500 µM of H_2O_2.

4.6.2 Comparison of activation by H_2O_2 X O_2 over time

To assess the time course of this process, the oxidized products were quantified over time under determined optimized settings in the absence and in the presence of H_2O_2 (Figure 14a). To investigate H_2O_2 accumulation in the reactions over time, the apparent H_2O_2 concentration was measured using Amplex Red reagent and horseradish peroxidase, as described in previosly reported protocols [59] (Figure 14b). It was observed that the product released was only grater for the system supllied with external H_2O_2 in the first 15 minutes of the reaction, after that, the reaction without the addition of external H_2O_2 is shown to have a greater accumulation of oxidized products. Also, it was possible to observe that before the flattening out of the products release presumably caused by the enzyme inactivation, the H_2O_2 levels were low and constant and a peak of H_2O_2 was observed shortly after the saturation of the products release (Figure 14b). This behaviour is similar to the one observed by Bissaro and colleagues.[68]

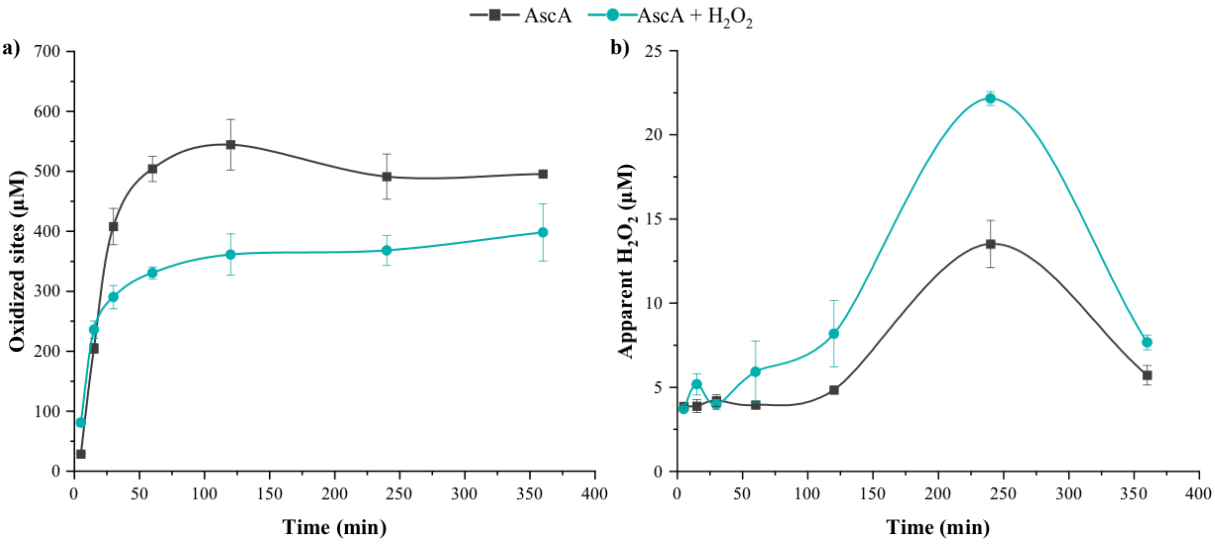

Figure 14 – Comparison of activation by H_2O_2 X O_2 over time. a) Evaluation of the use of H_2O_2 as a co-substrate over time for *Mt*LPMO9A (1 µM) using PASC as substrate assessed for the system with only ascorbic acid (1mM) and the system with ascorbic acid (1mM) in addition to H_2O_2 (50 µM); and b) The apparent H_2O_2 was measured over time for all the reactions using the coupled Amplex Red reagent and horseradish peroxidase reaction.
Source: By the author.

4.6.3 Evaluation of product generated under different conditions of oxygen sources

A deeper investigation on the co-substrate preference was performed in four different co-substrate conditions (±O_2 and ±H_2O_2, Figure 15). It was observed that in the system with low oxygen tension, it was not possible to identify product formation by *Mt*LPMO9A from PASC, demonstrating that presence of co-substrates is essential for the LPMO activity (Figure 15).

Addition of H_2O_2 in the oxygen-free environment in the presence of ascorbic acid led to complete restauration of enzymatic activity of the LPMO. The same occurs in the presence of oxygen and the absence of exogenous H_2O_2 (Figure 15). In other words, in the presence of 1mM of ascorbic acid *Mt*LPMO9A generate similar amounts of soluble oxidized products when either O_2 or H_2O_2 were present (Figure 15). The presence of both O_2 and H_2O_2 simultaneously generated a profile of soluble products a little less than when the two are present in isolation, as already shown for the time of 30 minutes in Figure 14. This happens because in this case H_2O_2 is being generated which together with the added H_2O_2 leads to inactivation of part of the enzyme population.

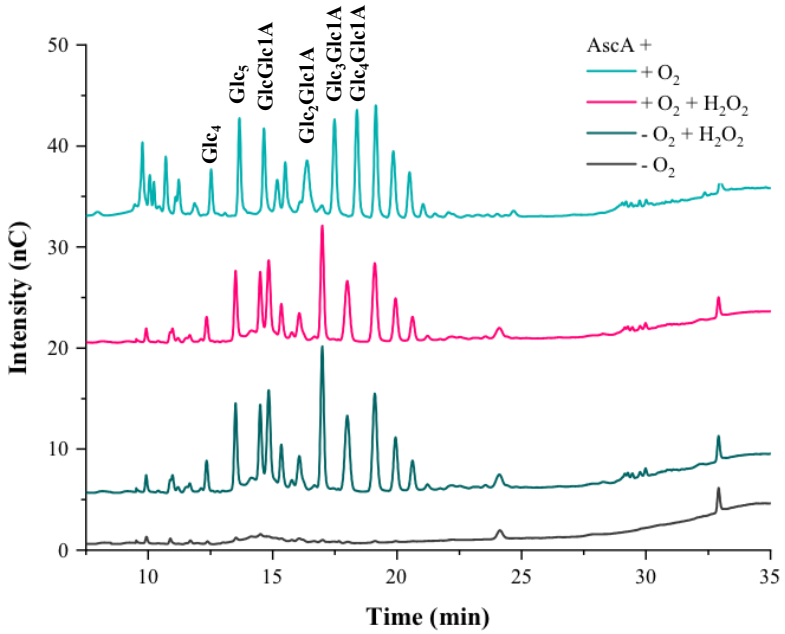

Figure 15 – Evaluation of *Mt*LPMO9A activity with and without oxygen and/or H_2O_2. To evaluate *Mt*LPMO9A (1 µM) activity on PASC $\pm O_2$ and $\pm H_2O_2$, the 30 minutes reactions were evaluated using ascorbic acid at 1mM concentration as a chemical electron donor.
Source: By the author.

4.7 Evaluation of *Mt*LPMO9A synergistic action with GH7 cellulases

When the first LPMOs were discovered and characterized, the commercial interest for these enzymes to act together with cellulases to improve the efficiency of enzyme cocktails was immediate.[69–71] However, it is known that LPMOs can have either a promoting or an impeding effect on these cellulases.[72–74] That fact leads to the need for individual evaluation of each enzyme.

Here, the synergistic action of *Mt*LPMO9A with two cellulases of *Trichoderma harzianum*, a cellobiohydrolase (Cel7A), and an endoglucanase (Cel7B), on cellulosic pulp was evalueted. BSA was used in control reactions to make it possible to carry out the individual sum of the enzyme's reactions. The result is shown in Figure 16, where it can be seen that the interaction of *Mt*LPMO9A with both cellulases resulted in a highly promoting effect.

The first reaction times showed a greater degree of synergism in the two reactions. For the Cel7A+*Mt*LPMO9A mixture, the first reaction hour showed a degree of synergism of 5.94, and an increase in product generated of 83.17%. For the Cel7B+*Mt*LPMO9A mixture, the degree of synergism observed for the first reaction hour was 6.25 with an increase in product release of 84%. After 6 hours of reaction, it was possible to observe that both systems

reached saturation, with a synergism degree of 1.71 and 1.61 for the system with Cel7A and Cel7B, respectively.

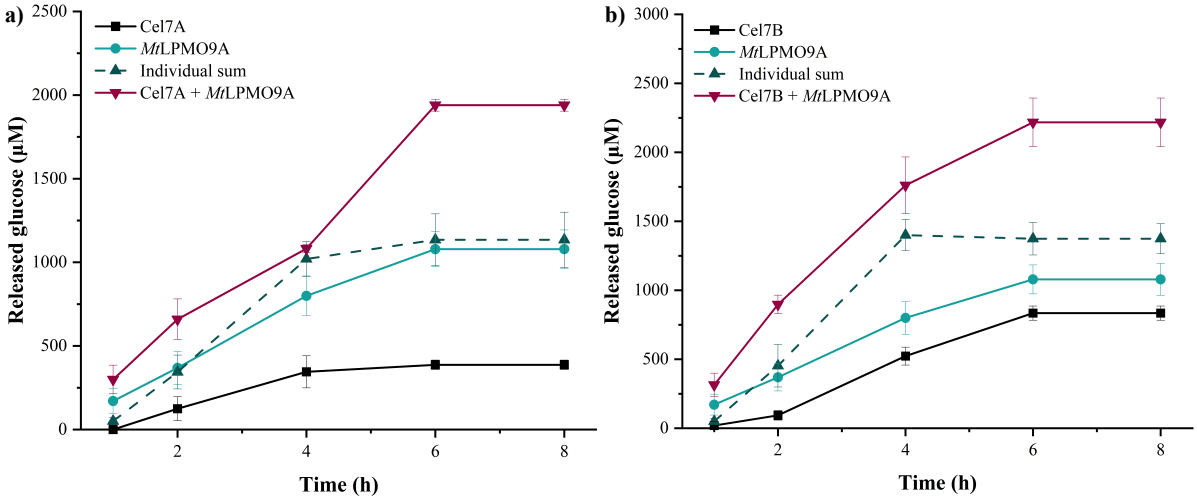

Figure 16 – Synergistic effect during cellulosic pulp degradation. a) Action of *Mt*LPMO9A in conjunction with Cel7A; b) Action of *Mt*LPMO9A together with Cel7B. Both reactions indicate a high degree of synergism and an increase in the production of generated products. The line represented the product formed in the interaction of the two enzymes (solid pink line linking inverted triangles), stands out for the sum and the individual reactions; although each line represents the same final amount of 1 mg of enzyme per gram of substrate.
Source: By the author.

Thus, *Mt*LPMO9A has a high potential to be used in commercial cocktails as it promotes a boost in the activity of traditional cellulases, significantly improving the performance of the system.

Chapter 5

Conclusions

In Part I of the present work, an LPMO from *Thermothelomyces thermophilus* M77 (formerly *Myceliophthora thermophila*) (*Mt*LPMO9A) was evaluated on the main aspects regarding the sequence, phylogeny, structure of the active copper site, use of cellulosic substrate, preference for reducing agent and mechanism pathways. Its synergetic action together with traditional cellulases, aiming at its biotechnological application, was also evaluated.

*Mt*LPMO9A proved to be an excellent target for study. Regarding its structure, it is a well-preserved enzyme of the AA9 family, presenting the histidine-brace and two aromatic amino acids (two tyrosines) in the active site that mimic the action of CBMs facilitating the binding of *Mt*LPMO9A to cellulosic substrates. Analyzing evolutionary distances, the *Mt*LPMO9A is placed close to enzymes with regioselectivity of C1 and C1/C4 oxidizing. When evaluating the real cleavage pattern, it was determined that, indeed, it does have a C1/C4 oxidation pattern but there is a prominent preference for C1 oxidation.

Regarding its biochemical characterization, a better performance of *Mt*LPMO9A was observed on the substrate of lower crystallinity, PASC, probably due to the fact that this substrate is more accessible to *Mt*LPMO9A. Besides, ascorbic acid reduces this *Mt*LPMO9A more efficiently than the other tested donor agents. *Mt*LPMO9A showed high structural stability over a wide pH range (5 to 10) where it has a high thermal stability of approximately 78°C. This high stability is highly desirable for industrial applications where extreme pHs are generally used [75-76] and also where LPMOs action is expected to be in conjunction with other cellulases that commonly have high temperatures for optimal activity.[77] Such characteristics combined with the evidence of great synergistic potential when evaluated together with traditional cellulases shown in the experiments, places *Mt*LPMO9A as a prominent target for biotechnological applications.

In addition to everything mentioned, it was also possible in this study to evaluate *Mt*LPMO9A as a function of one of the main sources of contradiction of LPMOs: the preferential mechanism of action of these enzymes. For *Mt*LPMO9A what has been demonstrated here is that the priming necessary for its activation with peroxide is high, and is not achieved with small amounts of reducers as demonstrated by previous studies. However, once this priming condition is optimized, the reaction with O_2 or without O_2, but with H_2O_2,

produces the same amount of products. This leads us to infer that *Mt*LPMO9A might not have a preferred source of co-substrate, using O_2 and H_2O_2 with equal efficiency. However, the reaction with H_2O_2 for longer times leads to saturation of the system as it inactivates the enzyme.

PART II:

The power of combining LPMOs and photocatalysis

Chapter 6

Introduction

Light is a ubiquitous and available source of energy that can be considered a key element of the modern bioeconomy. Photocatalytic degradation is a well-established field [78] and harnessing light energy to generate reactive oxygen species (ROS) using light-absorbing photosensitizers finds increasing and consolidated application in medicine (for example, for the treatment of cancer using photodynamic therapy, PDT).[79] Coupling the action of light in the photosensitizers generating activation in enzymes - the so-called photobiocatalysis - is an area that is still emerging.[80]

If we look especially at LPMOs, enzymes that need to be reduced (*i.e.,* needs an electron donor) and that can use ROS (*e.g.,* H_2O_2) in their mechanism cycle,[27,28] such coupling seems promising. For that reason, in Part II of the present work, it will be explored the light activation of *Mt*LPMO9A, using different photosensitizers and seeking to elucidate the reaction pathways involved. But before we start, let's take a closer look at the fundamental concepts of photobiocatalysis.

6.1 Photobiocatalysis

In the last 20 years, biocatalysis has established itself as a green tool in the pharmaceutical and chemical industry, as it is eco-friendly and allows reactions to occur in a specific and stereoselective way.[81-82] Progress in the field of directed evolution [83] has allowed the direct modification of enzymes and their adaptation to different reaction conditions, making the enzymes able to accept unnatural substrates, produce new products and even withstand extreme temperatures or pH values. All aiming to consolidate the use of enzymes in the most diverse industrial processes.[84]

In parallel with the consolidation of biocatalysis, photocatalysis has also become a broad field of investigation using (transition) metals or organic catalysts.[85–87] Another advance that further boosted photocatalysis was the discovery of several photosensitizers that

use visible light as an energy source.[87] All this combined with the fact that light can be obtained from electricity, generated from renewable energy sources, allows this process to be very eco-friendly.

It is not surprising then that the advances in these two areas would raise the question: *What would be the advantages of combining biocatalysis with photocatalysis?* And that is how photobiocatalysis emerged. Photobiocatalysis is currently carried out in three different ways: photocatalysis coupled to isolated enzymes or cell lysates containing enzymes of interest (Figure 17); photocatalysis applied to whole cells and photocatalysis applied to photoenzymes.[80] Since only a few known enzyme reactions require light alone, most transformations involving light and a biocatalyst exploit light to provide the co-substrate or cofactor in a redox state suitable for biotransformation.[84]

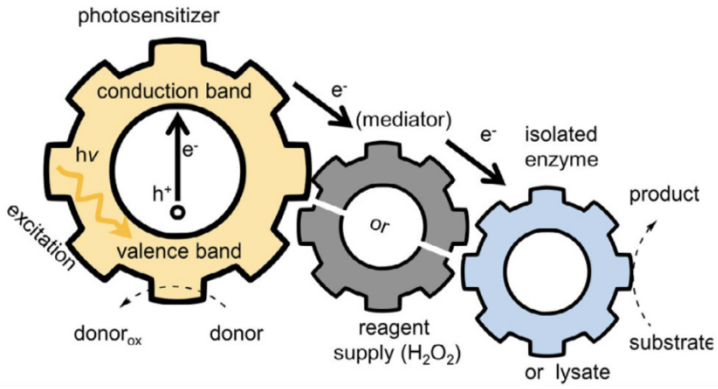

Figure 17 – Photobiocatalysis with isolated enzymes or lysate.
Source: SEEL; GULDER.[80]

6.2 LPMOs in photoactivated systems

The description of LPMOs being used in photocatalytic systems was first made in 2016, when independently Canella and Bissaro reported the application of photobiocatalysis to optimize the activity of LPMOs.[88-89] Cannela and co-authors showed that isolated thylakoids and chlorophyllin under light irradiation in the presence of ascorbic acid as a reductant were able to boost LPMO activity by two orders of magnitude.[88] Simultaneously, Bissaro *et al.* reported the use of vanadium-doped titanium dioxide (V-TiO_2) for LPMO activation.[89] More recently, Bissaro *et al.*[68] showed that the both of these systems can harness light and drive LPMO activity without the need for a reductant agent (*e.g.,* ascorbic acid). In 2020, Blossom and co-authors demonstrated that intermittent light irradiation can promote the structural disruption of cellulose equally well or better than continuous light irradiation.[90]

Despite such advances, the design of efficient photobiocatalytic systems able to promote the oxidative cleavage of recalcitrant polysaccharides such as cellulose is still representing a considerable challenge. For instance, only chlorophyllin[68,88,90] and TiO_2 [89] have been applied as photoelectron donors and there are no reports on the application of other classes of photosensitizing molecules to promote the photoactivation of LPMO.

6.3 Photoactivating molecules

As previously mentioned, the nature of the photosensitizer is also shown as an open area for extensive exploration. It is well established that photosensitizers commonly used in photodynamic therapy can transfer light energy to O_2 generating ROS or reactive molecular transients,[79,91–93] hence being potential targets for integrating photobiosystem with LPMOs.

The photochemical reactions developed by these photosensitizers proceed through two mechanisms called Type I and Type II, which occur simultaneously in the reaction medium in proportions depending on the photosensitizer used. Type I reactions generate radicals after the transfer of electrons from the triplet state to a substrate, such as molecular oxygen, leading to the production of superoxide anion ($O2^{\bullet -}$), hydroxyl radicals (•OH), and hydrogen peroxide (H_2O_2). In Type II reactions, the excited photosensitizer reacts directly with molecular oxygen (O_2) and forms the highly reactive singlet oxygen ($^1O_2$) through energy transfer [79,94-95] (Figure 18).

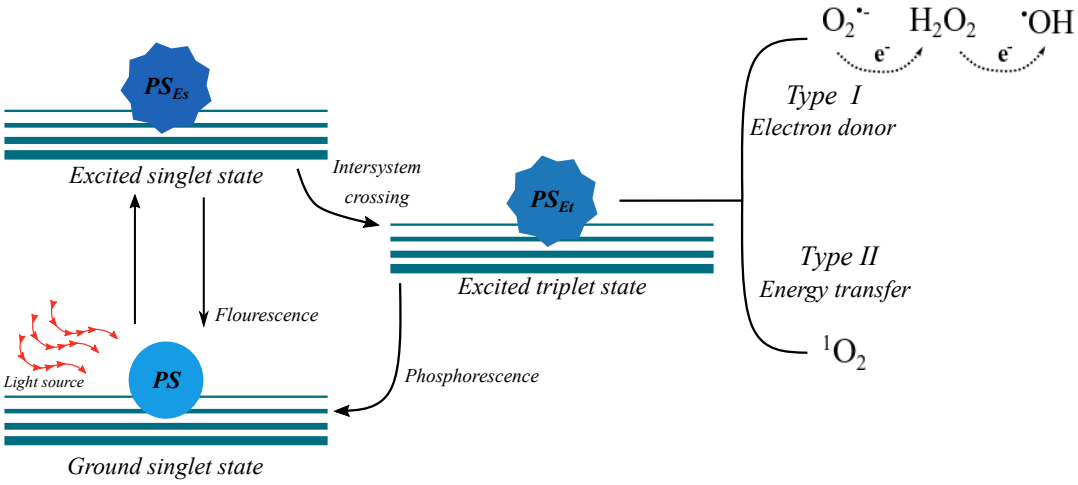

Figure 18 – Photoactivated photosensitizing molecules in its triplet state by undergoing two main pathways: type I (electron donor) and type II (energy transfer).
Source: By the author.

This process can be coupled to an enzymatic reaction, thus creating a photobiosystem.[80] In particular, in the case of LPMOs, this union not only provides electrons necessary for the reduction of LPMO-Cu (II) in LPMO-Cu (I) but also provides H_2O_2, which can be used in its mechanism. Hence, the analysis of the feasibility of using these other photosensitizers can mean an advance in photoactivated systems with LPMOs.

Chapter 7

Objectives

7.1 Overall objectives

The overall Part II objective consists of *Mt*LPMO9A as an integrant of photobiosystem. The analysis will start with the most commonly used photosensitizer chlorophyllin, passing then to a common PDT photosensitizer, methylene blue. Their reaction intermediates will be evaluated as well as the stability of the system.

7.2 Specific objectives

- Evaluation of the use of chlorophyllin from reactions with *Mt*LPMO9A and comparison with the reaction triggered only by ascorbic acid
- Determination of the co-substrate use by the system
- Characterization of methylene blue as a photosensitizer capable of integrating a photobiosystem with *Mt*LPMO9A
- Analysis of reaction intermediates for the system *Mt*LPMO9A/methylene blue.

Chapter 8

Material and methods

This Chapter focuses on specifying the different methodology used in Part II of the present work. Topics such as expression and purification of *Mt*LPMO9A, and analysis of products generated via HPAEC are as described in Chapter 3 and will not be repeated here.

8.1 Home-made Light Systems

For the activation of photosensitizers, one photosystem (Biotable® apparatus, São Carlos Institute of Physics, São Carlos, SP, Brazil) was built in order to activate them efficiently. The photosystem had a heat dissipation system, ensuring the stability of the reaction system, and consisted of LEDs at the frequency of 660 nm and irradiance of 50 mW/cm^2.

8.2 Chlorophyllin as photosensitizer

8.2.1 Standard reaction for chlorophyllin light-induced assays

The standard basis for chlorophyllin light-induced enzymatic reaction was 1μM of *Mt*LPMO9A, 500 μM of chlorophyllin in sodium phosphate buffer, pH 6.0, at 50 ^oC and 1000 rpm. To enable light transmission, reactions were performed in a 2mL Eppendorf tube (Eppendorf, Hamburg, Germany) sealed with Parafilm^R M (Sigma-Aldrich, St. Louis, USA). The reactions were initiated by adding the photosensitizer to the reaction followed by the light activation and, in experiments conducted in the presence of AscA, its addition was performed simultaneously with the light activation of chlorophyllin.

8.2.2 Evaluation in PASC over time

Using PASC 0.3 % (w/v) as substrate, it was performed an evaluation of the generated products over time at 5 min, 15 min, 30 min, 1 hour, 2 hours, 4 hours and 6 hours. The evaluated systems were *Mt*LPMO9A+1mM AscA, *Mt*LPMO9A+1mM AscA+ 500 μM of chlorophyllin and *Mt*LPMO9A+500 μM of chlorophyllin.

8.2.3 Evaluation of the photobiosystem in Avicel

To evaluate Avicel as substrate in this photobiosystem, it was used the final concentration of 1.0% (w/v) of this substrate, in 4 hours reactions. The evaluated systems were *Mt*LPMO9A+1mM AscA, *Mt*LPMO9A+1mM AscA+500 μM of chlorophyllin and *Mt*LPMO9A+500 μM of chlorophyllin.

8.2.4. Evaluation of product generated under different conditions of oxygen sources

The role of O_2 and H_2O_2 as oxygen source was evaluated under N_2 atmosphere, using PASC substrate in the *Mt*LPMO9A+1mM AscA+ 500 μM of chlorophyllin and *Mt*LPMO9A+500 μM of chlorophyllin systems. To confirm that the enzymatic reactions were performed under low oxygen tension, the O_2 pressure was measured using the NeoFox optical oxygen sensor (OceanOptics). When present, H_2O_2 was added in a 50 μM final concentration. These reactions were performed for 30 minutes.

8.3 Methylene blue as photosensitizer

8.3.1 Standard reaction for methylene blue light-induced assays

In a 2 mL Eppendorf tube (Eppendorf, Hamburg, Germany) sealed with Parafilm^R M (Sigma-Aldrich, St. Louis, USA) to enable light passage, the standard basis for enzymatic reaction was 1 μM of *Mt*LPMO9A mixed with 0.3% (w/v) of PASC and a 20mM ABF pH 9; reactions were conducted at 50 ºC and 1000 rpm for 4 hours (unless state otherwise). Methylene blue began to be used at a concentration of 500 μM, and then had its ideal concentration standardized as 10 mM. The reactions were initiated by adding the photosensitizer to the reaction followed by the activation of light. In experiments conducted in the presence of AscA, its addition was made simultaneously with the activation of the photosensitizer.

8.3.2 Assessments of the ideal conditions for the functioning of the photobiosystem

The reaction parameters evaluated for this photobiosystem were: pH, temperature, photosensitizer concentration and light incidence concentration. To evaluate the pH, it was

varied in a range from 2 to 10 using ABF buffer, using the standard temperature of 50 ºC. Then, it was evaluated the generated products at the temperature of 30 ºC, 40 ºC and 50 ºC. Both physical parameters mentioned were evaluated at a concentration of 500 µM of methylene blue.

Then, the determination of the ideal photosensitizer concentration was performed. Concentrations of 500 µM, 1 mM, 2 mM, 5 mM, 8 mM, 10 mM, 15 mM, and 20 mM were evaluated. Then, fixing the concentration at 10 mM, the influence of the amount of irradiated light was evaluated, allowing 33.3%, 66.6% and 100% light to pass through.

8.3.3 Synergistic action with ascorbic acid

It was also performed a comparative analysis of methylene blue in the presence of varying concentrations of ascorbic acid (0, 0.1, 0.5 and 1mM) for 30 minutes, 2 and 4 hours, with the activation with 1mM of ascorbic acid. Reactions occurred at the standard conditions.

8.3.4 Evaluation of product generated under different conditions of oxygen sources

The role of O_2 and H_2O_2 as oxygen source for *Mt*LPMO9A/methylene blue photobiosystem was evaluated under N_2 atmosphere, using PASC substrate. To confirm that the enzymatic reactions were performed under low oxygen tension, the O_2 pressure was measured using the NeoFox optical oxygen sensor (OceanOptics). When present, H_2O_2 was added in a 50 µM final concentration. These reactions were performed for 1 hour.

8.3.5 Further investigations on Methylene blue/ *Mt*LPMO9A reaction intermediates

8.3.5.1 $NaHSO_3$ as H_2O_2 scavenger

A more specific investigation of the reaction intermediates was done through the addition of $NaHSO_3$ to the photobiosystem. First, the concentrations of 0.5 mM, 1 mM, 5 mM, 10 mM and 50mM of this compound were added to the *Mt*LPMO9A/methylene blue system in a one-hour reaction. To ensure that these concentrations did not interfere with the integrity of the enzyme and that the result obtained was due to interferences in the reaction cycle, two tests were carried out:

i) Residual activity. *Mt*LPMO9A was incubated for 1 hour with the mentioned $NaHSO_3$ concentrations and then the compound was removed with buffer exchange by centrifugation. With the pure enzyme, an overnight reaction was performed and the products were evaluated.
ii) Analysis of structure integrity by Thermofluor. A Thermofluor test similar to that presented in section 3.4 was performed. The differences were that in this test the pH was kept fixed at 9 and the mentioned concentrations of $NaHSO_3$ were added.

The relationship between the amount of $NaHSO_3$ and the consumption of H_2O_2 was measured using the previosly reported protocol [59] that uses Amplex Red reagent and 7.1 U mL^{-1} horseradish peroxidase (both from Sigma-Aldrich). The mesurement was performed at 30 ºC in a spectrophotometer at 563 nm.

8.3.5.1 Evaluation over time

The concentration of 0.5 mM of $NaHSO_3$ was evaluated over time and compared with the reaction without the addition of this component. The evaluated times were: 30 minutes, 1 hour, 2 hours, 4 hours, 6 hours, 8 hours and 16 hours.

Chapter 9

Results and discussion

9.1 Chlorophyllin as photosensitizer

9.1.1 Evaluation in PASC over time

The first assessment of the use of light to activate *Mt*LPMO9A started with the use of chlorophyllin, a photosensitizing molecule commonly used in the literature as a member of photobiosystems along with LPMOs.[68,88,90] This evaluation was carried out using PASC as a substrate over time. As a result, it was observed that for the first reaction times the photoactivation system coupled with ascorbic acid is very efficient, leading to a strong stimulation of *Mt*LPMO9A activity (Figure 19).

However, evaluation for longer reaction times showed that the photoactivated coupled system led to a product-release saturation faster than the ascorbic acid-driven reaction, indicating an early inactivation of the enzyme under conditions of photoactivation (Figure 19b). This is more probably a result of H_2O_2 formation in the photoactivation process, which, in high concentrations, lead to *Mt*LPMO9A inactivation.[68] Nevertheless, *Mt*LPMO9A under the photoactivation conditions shows highly efficient product release at the short reaction times. When photoactivated system (*Mt*LPMO9A+chlorophyllin+light) was decoupled from the ascorbic acid, the product formation was considerably decreased (Figure 19b). This result is orthogonal to recent observations of Bissaro and colleagues[68] and indicates that *Mt*LPMO9A, in the absence of ascorbic acid, is not as efficiently activated by the H_2O_2 produced by light-activated chlorophyllin as the previously studied LPMOs.[68] Since in the absence of chemical reductant, ascorbic acid, LPMO-mediated cellulose oxidation proceeds at a much slower pace, one can conclude that electron donation to the LPMO, either directly by chlorophyllin or via generated superoxide ion, is inefficient for *Mt*LPMO9A (Figure 19).

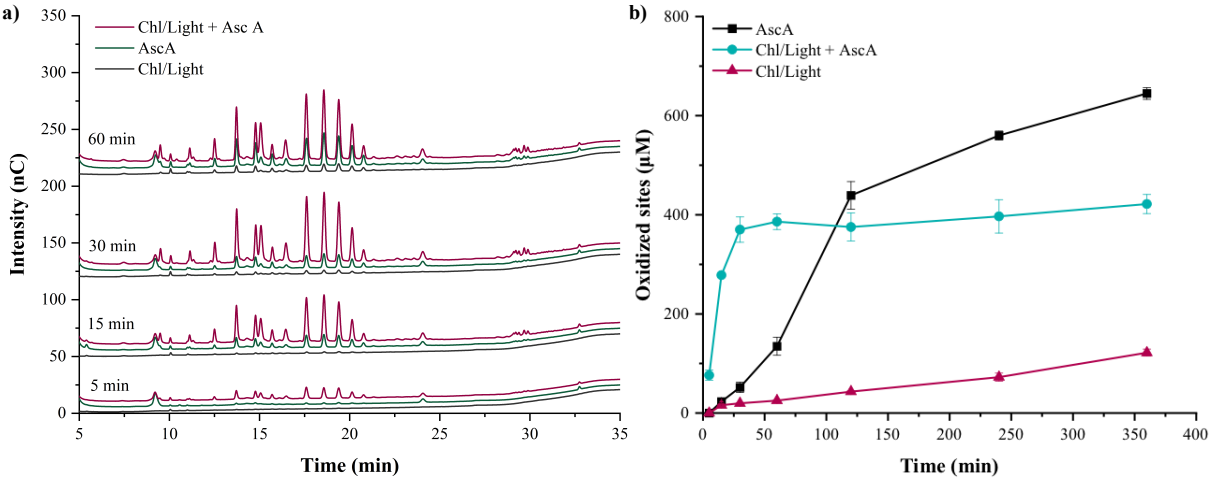

Figure 19 – Evaluation light boost effect on *Mt*LPMO9A (1 µM) activation. a) Chromatograms for 5 minutes, 15 minutes, 30 minutes, and 60 minutes showing the predominance of products formed at the photoactivated system that couples chlorophyllin and ascorbic acid. b) Quantitative evaluation of the generated oxidized products as a function of time. Reactions were performed using PASC as substrate.
Source: By the author.

9.1.2 Evaluation of the photobiosystem in Avicel

Next, it was evaluated whether the presence of light mediated by chlorophyllin would stimulate *Mt*LPMO9A activity on more recalcitrant substrates. The products generated from Avicel at 1% (w/v) were evaluated at the end of 4 hours of reaction. The presence of light-activated chlorophyllin significantly increased the products release by *Mt*LPMO9A, indicating a considerable boost of its activity on the more crystalline substrates (Figure 20). Thus, *in situ* H_2O_2 production by the photoactivated chlorophyllin [68,79] in the presence of chemical reductant can boost *Mt*LPMO9A activity on the more crystalline and recalcitrant substrate.

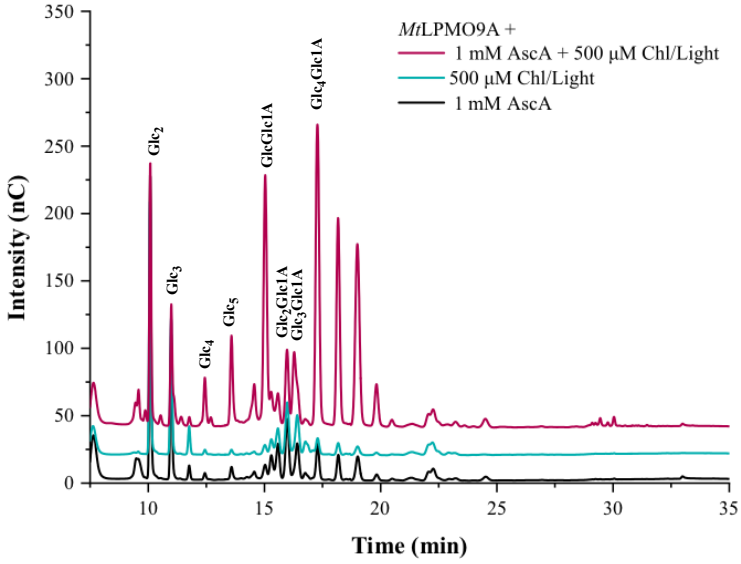

Figure 20 – Change in *Mt*LPMO9A (1 µM) performance in the presence of light and chlorophyllin. The photoactivated system increased the enzyme's activity on Avicel, a substrate with a higher degree of crystallinity. The marked standards represent: Glc2: cellobiose, Glc3: cellotriose, Glc4: cellotetraose, Glc5: cellopentaose; C1-oxidized oligosaccharides are represented as: GlcGlc1A: cellobionic acid, Glc2Glc1A: cellotrionic acid, Glc3Glc1A: cellotetraonic acid, Glc4Glc1A: cellopentaonic acid.
Source: By the author.

9.1.3 Evaluation of product generated under different conditions of oxygen sources

Finally, evaluation of the role of co-substrates (O_2 and H_2O_2) when *Mt*LPMO9A is activated by light in the presence of chlorophyllin was performed. Analysis of chlorophyllin-only photoactivated system (Figure 21a), shows once a lack of products formation at the absence of co-substrates (H_2O_2 and O_2) and chemical reductant. Presence of either H_2O_2 or O_2 resulted in a small quantity of products. Simultaneous presence of oxygen and exogenous H_2O_2 resulted in higher quantities of soluble products, which, however, was still significantly smaller than that observed in the coupled presence of chemical reductant (AscA; Figure 21b). Limited catalytic activity of *Mt*LPMO9A in the system with low oxygen tension and exogenous H_2O_2 or in the presence of molecular oxygen reveals that chlorophyllin-activation has a low capacity of *Mt*LPMO9A reduction (either via direct electron transfer or via superoxide ion, $O_2^{\bullet-}$), an opposite to what was recently shown by Bissaro and co-workers.[68] The reason for this is currently not clear, but the observed differences could be related to different LPMOs which were studied or the differences in the applied experimental conditions.

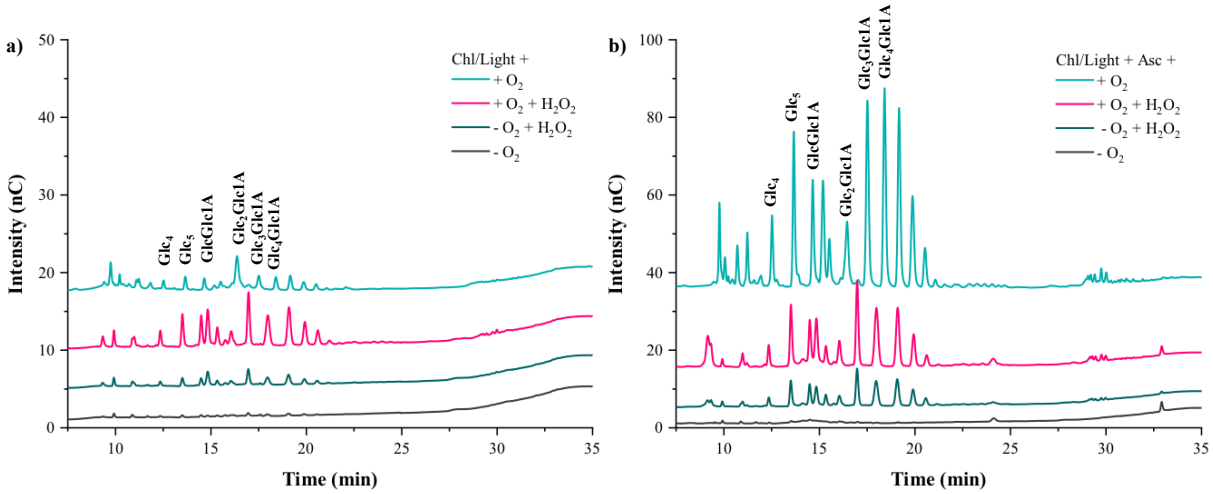

Figure 21 – Evaluation of *Mt*LPMO9A activity with and without oxygen and/or H_2O_2. To evaluate *Mt*LPMO9A (1 µM) activity on PASC ±O_2 and ±H_2O_2, the 30 minutes reactions were evaluated under different settings: a) Photoactivated system with 500µM of chlorophyllin, and b) coupled photoactivated system that combines 1mM of ascorbic acid with 500µM of chlorophyllin. The marked standards represent: Glc4: cellotetraose, Glc5: cellopentaose; C1-oxidized oligosaccharides are represented as: GlcGlc1A: cellobionic acid, Glc2Glc1A: cellotrionic acid, Glc3Glc1A: cellotetraonic acid, Glc4Glc1A: cellopentaonic acid.

Source: By the author.

Finally, we investigated a role of chemical reductant (ascorbic acid) coupled with chlorophyllin in the LPMO activation. Except for a trivial case of a lack of products in the absence of any oxygen source, the photoactivated system that couples light-activated chlorophyllin and ascorbic acid has a more complex interpretation (Figure 21b). It was observed that the products are increasing towards the low oxygen tension system supplied with exogenous H_2O_2 to regular oxygen tension supplied with exogenous H_2O_2, reaching the maximum release of products at no exogenous H_2O_2 and normal oxygen tension condition (Figure 21b).

Since in this system *Mt*LPMO9A can be considered to be in reduced form, the first two previously mentioned situations (low oxygen tension system supplied with exogenous H_2O_2 and regular oxygen tension supplied with exogenous H_2O_2) shows that *Mt*LPMO9A acts via the peroxygenase pathway. But the fact that products released raised with the presence of O_2 show that *Mt*LPMO9A has a high action via the monooxygenase pathway, which can be mainly amputated by the protonation of distal oxygen (where no H_2O_2 intermediate is required)[28] (Figure 21b).

Moreover, the fact that the enzyme has a superior performance in the system with only oxygen (Figure 21b) demonstrates that we are visualizing a moment where the formed H_2O_2 in addition to the exogenous H_2O_2 led to the excess of this reagent in the reaction medium causing the enzyme inactivation.

9.2 Methylene blue as photosensitizer

Methylene blue is a hydrophilic phenothiazine derivative with a strong absorption between 550-770 nm, which displays a maximum molar absorptivity of 85,000 M^{-1} cm^{-1} at 664 nm. It is widely used for PDT, and preferentially works by type I mechanism (electron transfer).[96]

9.2.1 Assessments of the ideal conditions for the functioning of the photobiosystem

To assess the potential of methylene blue as a photosensitizer capable of mediating light-activation of *Mt*LPMO9A, a reaction PASC was performed for 16 h, at 50 °C in 20 mM sodium citrate pH 5. Methylene blue diluted in water at a concentration of 500 µM was used. Significant photo-activation of *Mt*LPMO9A was observed leading to the formation of oxidized products in the absence of any external reducing agent (Figure 22).

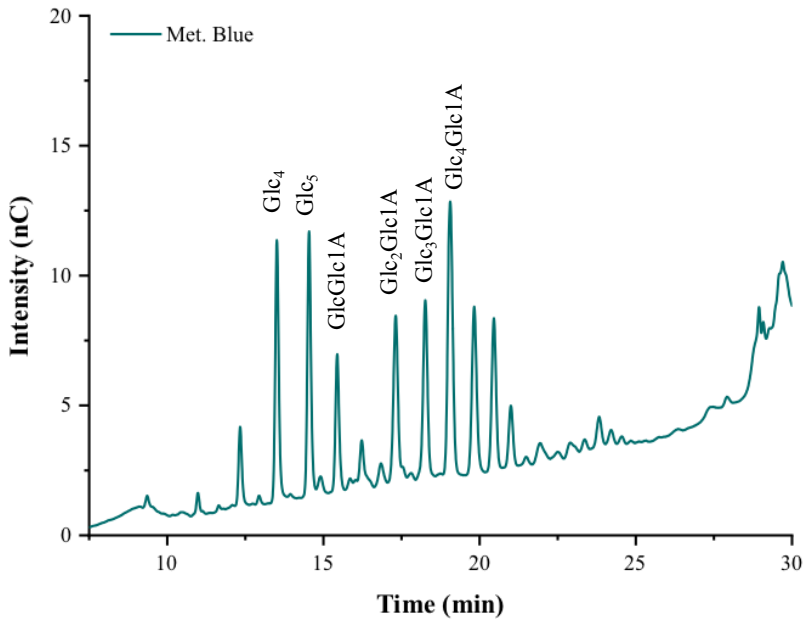

Figure 22 – Assessment of the ability of methylene blue to activate *Mt*LPMO9A at the absence of chemical reductant. The marked standards represent: Glc_4: cellotetraose, Glc_5: cellopentaose; C1-oxidized oligosaccharides are represented as: GlcGlc1A: cellobionic acid, Glc_2Glc1A: cellotrionic acid, Glc_3Glc1A: cellotetraonic acid, Glc_4Glc1A: cellopentaonic acid.
Source: By the author.

Further analysis of the photobiosystem were performed to determine the optimal conditions of the LPMO-photosensitizer coupling. The first parameter to be optimized was the pH of the reaction. The enzyme is known to act at pH 5 [61-62] whereas methylene blue has the highest quantum yield of the triplet state in the condition at pH 9.[97] Optimization reactions

were performed at PASC in different pHs using acetate/borate/sodium phosphate (ABF) buffer at 50 °C, for 4 hours. Analysis of the generated products showed that the photobiosystem provides a higher rate of product formation as the reaction conditions become more alkaline, with an increasing efficiency starting at pH 6, and reaching its maximum at pHs 8 and 9 (Figure 23a).

Another fundamental parameter to be determined is the system operating temperature. *Mt*LPMO9A has been reported to be active at 50 °C,[61-62] but it is well-known that the formation of reactive oxygen species is temperature-dependent.[98] Therefore, an evaluation of how the coupled system would respond to the temperature variations was performed. The optimum pHs of the LPMO photoactivation, pH 8 and 9, were explored. It was observed that products formation is temperature-dependent, raising from 30 °C to 50 °C in 4 hour reactions (Figure 23b).

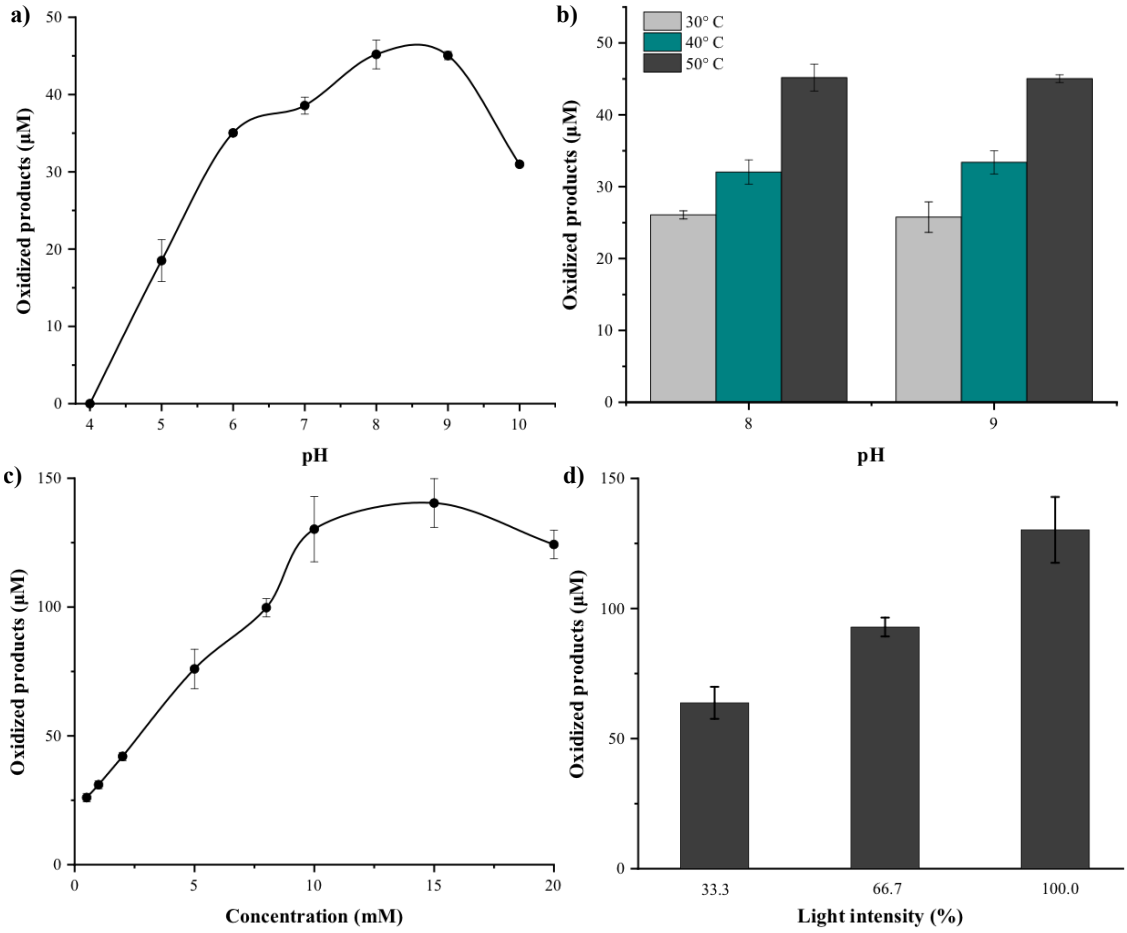

Figure 23 – Optimization of methylene blue/ *Mt*LPMO9A photobiosystem. Determination of the best performance a) pH and b) temperature of the photobiosystem; These experiments were performed in 4 hours reactions using 500 µM of methylene blue. The assessment of the influence of concentrations of c) methylene blue and d) incident light on the release of oxidative products released from PASC were performed. These experiments were also performed in 4 hours reaction with 1µM of *Mt*LPMO9A at 50 °C pH 9. The light intensity experiments were performed with the optimum 10mM concentration of methylene blue.

Source: By the author.

After determination of the optimal pH and temperature conditions for the studied photobiosystem, we move on to determine methylene blue concentration that led to the most efficient oxidative products formation (Figure 23c). The products release as a function of methylene blue concentration shows that the yield of oxidized products is highest at 10 mM of methylene blue. Since light plays a fundamental role for a photobiosystem activation, the efficiency of the LPMO methylene blue activation was analyzed by varying the light irradiance up to its maximum value of 50 mW/cm^2 (Figure 23d). The amount products generated by the system increases linearly with an increase in light intensity.

9.2.2 Synergistic action with ascorbic acid

The use of ascorbic acid is a classical approach to activate LPMOs.[11,62-63,99-100] Pioneer studies that made use of photosensitizers to boost LPMO activity were carried out also in the presence of this electron donor.[68,88] Thus, this traditional approach was followed here to compared the activity of methylene blue in the presence of varying concentrations of ascorbic acid (0, 0.1, 0.5 and 1mM) for different periods of time (30 minutes, 2 and 4 hours) as well as with the widely used activation with 1mM of ascorbic acid at the absence of methylene blue (Figure 24).

In the presence of methylene blue, increasing concentrations of ascorbic acid caused a continuous increase in the released oxidative products during the first 30 minutes of reaction (Figure 24). However, a saturation in the LPMO products release occurred from 0.5 mM of ascorbic acid and higher for 2 and 4 hours reactions (Figure 24). This means that, for longer times, the addition of 0.5 or 1mM of ascorbic acid to the reaction did not have any beneficial effect. For the short time periods (30 minutes) reactions with an addition of 0.5 and 1mM of ascorbic acid generated more products than the standard LPMO reaction with 1mM of ascorbic acid.

This fact is in line with what was observed previously for photoactivated systems that also showed higher product release rates for the short reaction times [68,88] and also in line with the previous results using chlorophyllin. However, for longer reaction times, the system where only ascorbic acid was present leads to the formation of more products presumably because the enzyme remains active for a longer time.

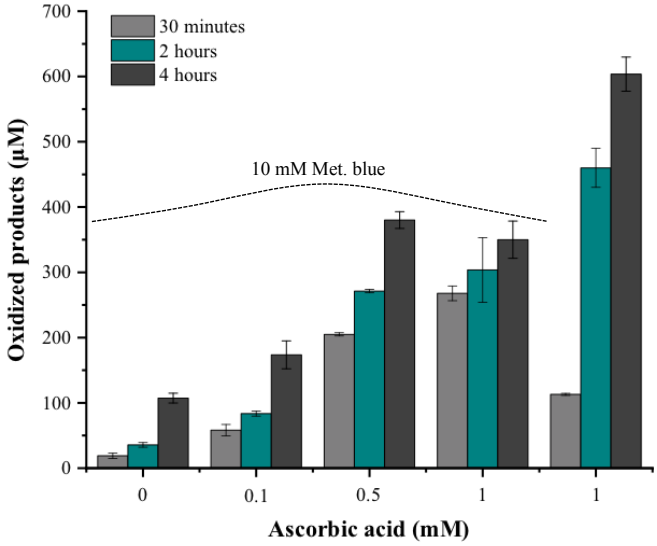

Figure 24 – Synergistic effect of photosensitizers with ascorbic acid. Figure shows the LPMO-generated oxidized product released in 30 min, 1 hour and 4 hours reactions in the presence of 10 mM of methylene blue with different concentrations of ascorbic acid (first four trios of columns) and also the system without methylene blue with 1mM of AscA (last trio of columns).
Source: By the author.

9.2.3 Evaluation of the photobiosystem under different conditions of oxygen sources

As performed for the other systems so far, the evaluation of the role of co-substrates (O_2 and H_2O_2) was performed for methylene blue + *Mt*LPMO9A photobiosystem. The experiments were performed at the presence and/or absence of O_2 (under N_2 atmosphere in the latter case) evaluating the influence of H_2O_2 addition (at final concentration of 50 µM) for each of the previous conditions. Reactions occurred for 1 hour, at 50 °C and 1000 rpm.

The resulting chromatograms allow the inference about the interactions of the components of this photobiosystem (Figure 25). Starting with the trivial case, at the absence of oxygen and hydrogen peroxide ($-O_2$-H_2O_2) there was no formation of oxidative products. When the oxygen and external reductant were absent, but H_2O_2 was present ($-O_2$+H_2O_2), the products formation occurred. This indicates that methylene blue is capable of reducing *Mt*LPMO9A via direct electron transfer. This result also shows that the products formation occurred via peroxygenase pathway.

However, when both co-substrates, O_2 and H_2O_2, or when only O_2 are supplied to the system, the amount of oxidated products produced by the LPMO is much higher than the previously observed but they are very similar with each other. This may be directly related to two factors: (1) more LPMOs are being reduced in the reaction medium since in the presence of O_2 there is a conversion of O_2 to $O_2^{\bullet-}$ by methylene blue, and (2) even when only O_2 is presented, H_2O_2 is being produced by methylene blue through the electron donor route, hence

in both cases (+ O_2 + H_2O_2 or + O_2 - H_2O_2) product formation is taking place both via the peroxygenase and monooxygenase pathways, indicating that these are actually complementary routes and also that in the former case, the exogenous H_2O_2 makes no difference in the system.

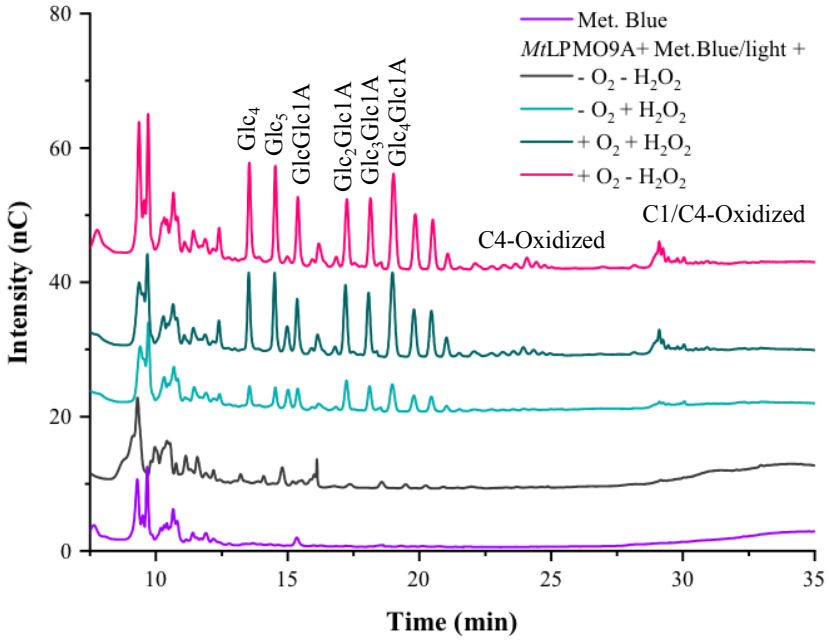

Figure 25 – Qualitative analysis of the influence of oxygen source at the photobiosystem. Reactions contained 10 mM methylene blue and 1 µM of *Mt*LPMO9A (when present) for 1 hour, 50 °C, 1000 rpm, pH9 under different co-substrate conditions. The chromatogram in pink shows a control system with methylene blue but without *Mt*LPMO9A, the dark gray curve represents the final products of the LPMO reaction in an anoxic environment, the cyan green curve shows the oxidative products when 50 µM of H_2O_2 was added to the reaction and lastly, the dark green represents the product formation when both O_2 and H_2O_2 were present in the reaction medium.
Source: By the author.

9.2.4 Further investigations on Methylene blue/ *Mt*LPMO9A reaction intermediates

To go further on the investigation into the mechanism of action of the components of this photobiosystem, as well as the chemical intermediates involved, we carried out experiments to determine the effect of suppression of H_2O_2 on the reaction. For that we used sodium bisulfite ($NaHSO_3$) as an H_2O_2 scavenger. This process occurs because H_2O_2 oxidizes SO_3^{2-} releasing SO_4^{2-} and H_2O.[101–103]

9.2.4.1 $NaHSO_3$ as H_2O_2 scavenger

First, a quantitative analysis of the concentrations of $NaHSO_3$ used and related it to the H_2O_2 consumption was performed. Lower concentrations of $NaHSO_3$ lead to a modest

consumption of H_2O_2, however, higher $NaHSO_3$ concentrations remove significant amounts of H_2O_2 (Figure 26).

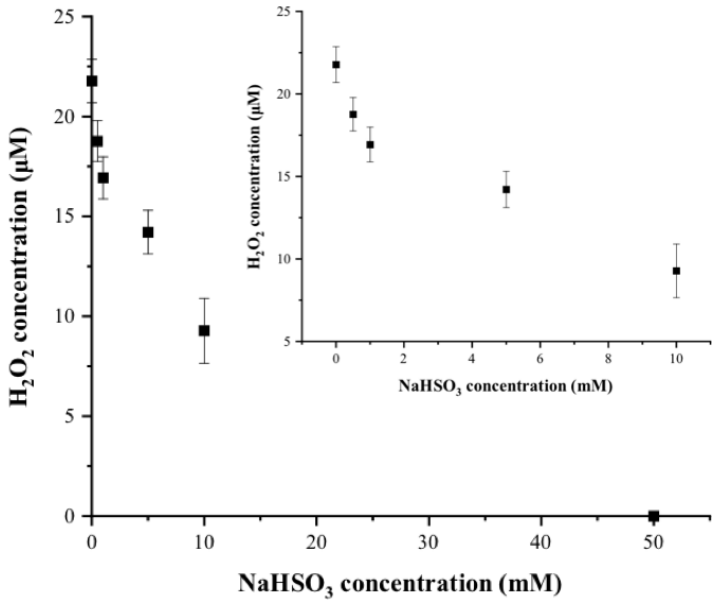

Figure 26 – Relationship of $NaHSO_3$ concentration with H_2O_2 consumption. The apparent H_2O_2 was measured using the coupled Amplex Red reagent and horseradish peroxidase reaction.
Source: By the author.

Then, it was assessed the influence on the oxidized products generated by the addition of different concentrations of $NaHSO_3$. An increase in the amount of LPMO oxidation products was observed for small concentrations of $NaHSO_3$ (0.5 and 1mM) followed by a sharp decrease in the enzyme activity at higher $NaHSO_3$ concentrations. (Figure 27).

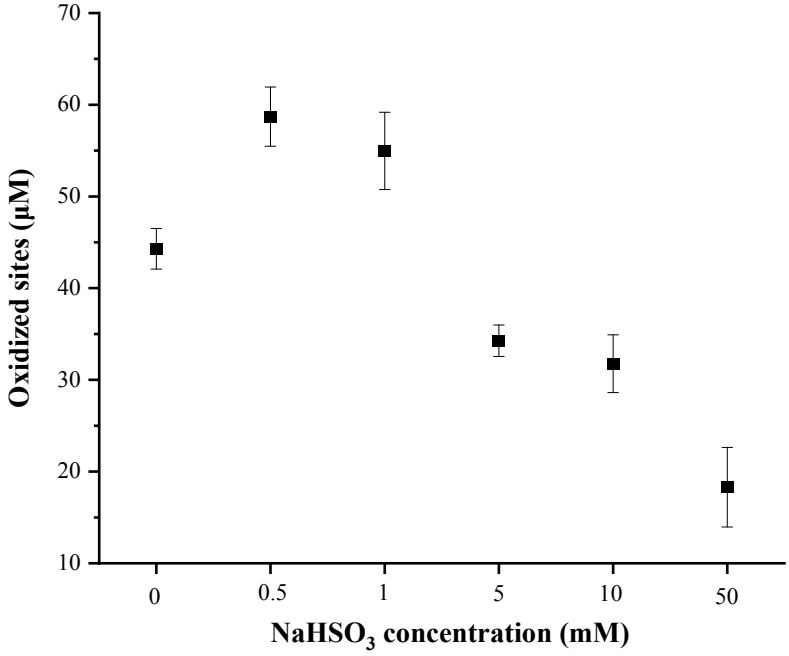

Figure 27 – Evaluation of the products generated in a 1 hour reaction with different concentrations of $NaHSO_3$.
Source: By the author.

Control experiments of the viability of *Mt*LPMO9A under higher $NaHSO_3$ concentrations following both residual activity and the enzyme structural integrity using a thermal shift assay revealed that $NaHSO_3$ does not interfere significantly within the viability of the enzyme and its selectivity (Figure 28). Therefore, it can be inferred that the decrease in the products released observed in Figure 25 for high concentrations of $NaHSO_3$ is directly related to H_2O_2 consumption in the reaction medium, once higher $NaHSO_3$ concentrations remove significant amounts of H_2O_2 (Figure 26). In this case, the effect of $NaHSO_3$ on the enzymatic activity becomes unproductive, since a decrease in the co-substrate (H_2O_2) availability directly interfered with the peroxygenase pathway, decreasing generation of oxidative products by the LPMO.

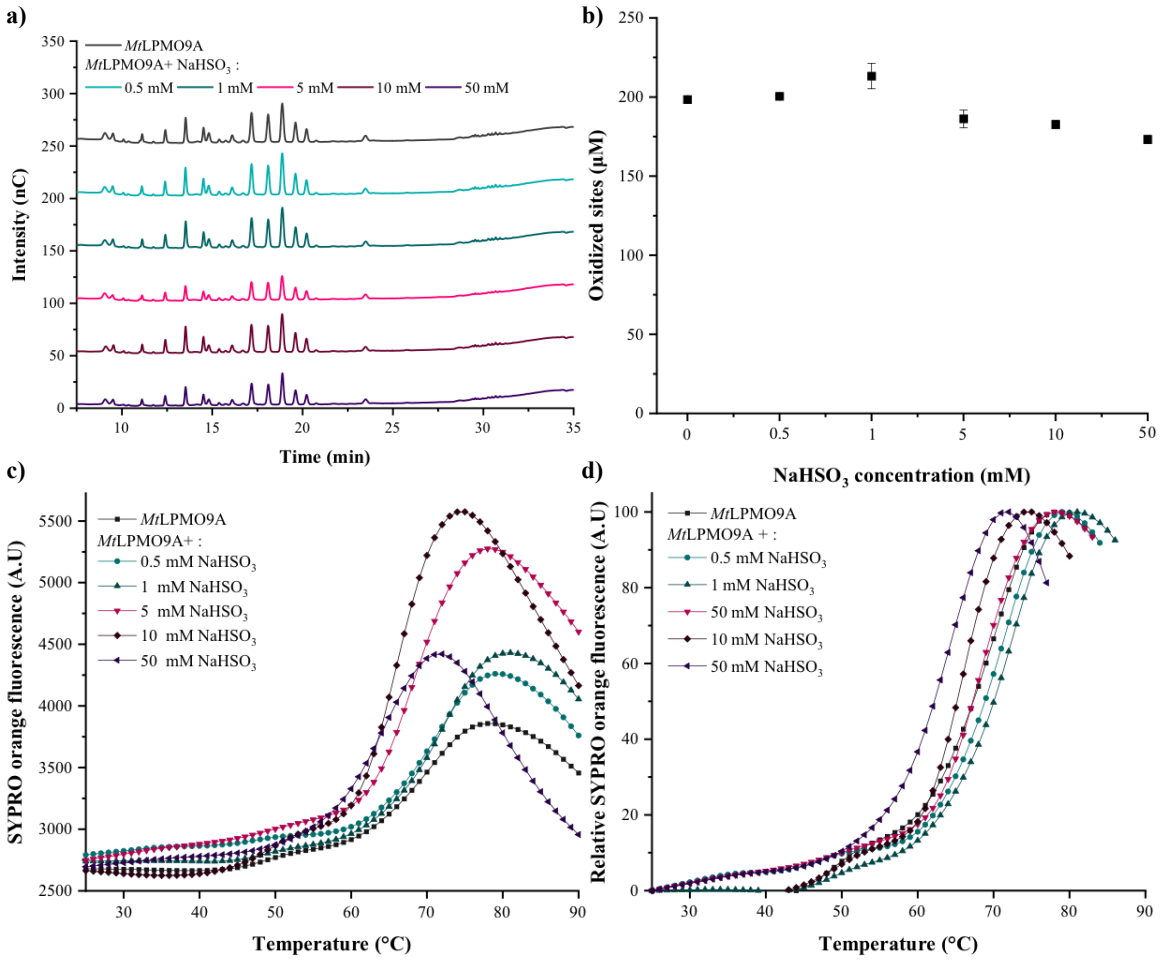

Figure 28 – Evaluation of enzymatic viability in the presence of different concentrations of $NaHSO_3$. The LPMO viability was first evaluated by measuring of its residual activity. As can be seen in the a) chromatographs and b) quantitative oxidative products measurements, there was no significant difference in the activity of the enzyme submitted to different $NaHSO_3$ concentrations. Enzymatic viability was also analyzed using a thermal shift assay. c) SYPRO orange fluorescence and d) the relative SYPRO orange fluorescence. The concentrations of 5, 10 and 50 mM of $NaHSO_3$ shows a slight shift in the denaturation temperature but nothing significant to *Mt*LPMO9A inactivation.
Source: By the author.

9.2.4.2 Evaluation over time

*Mt*LPMO9A activity in the presence of methylene blue and presence or absence of 0.5mM of $NaHSO_3$ as a function of time was then evaluated. Figure 29 shows the expressive increase in the accumulation of LPMO-generated oxidative products over time, indicating that the $NaHSO_3$ in the optimized concentration is an important ally of the photoactivated LPMO, which provides significant improvement in its efficiency.

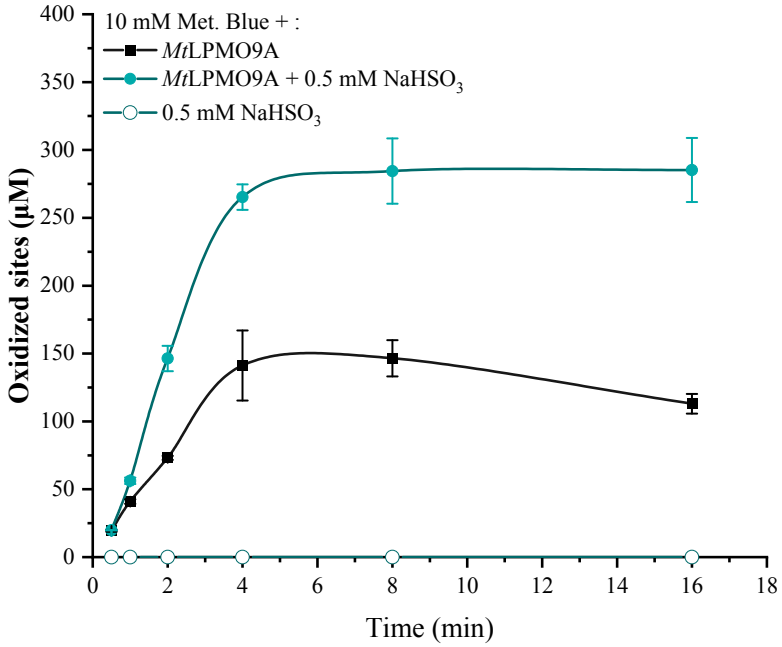

Figure 29 – Quantitative analysis of products generated over time by the system with (green line) and without (black line) the addition of 0.5mM $NaHSO_3$.
Source: By the author.

Chapter 10

Conclusions

In Part II of the present work, the ability of *Mt*LPMO9A to integrate photobiosystems in the presence of two photosensitizers, chlorophyllin, and methylene blue, was evaluated. Chlorophyllin has been used previously in the literature to activate LPMOs.[68,88,90] Regarding the activation of *Mt*LPMO9A, it was observed that chlorophyllin alone did not show to be able to efficiently activate the enzyme. But when coupled with ascorbic acid it provided a significant boost for the first reaction times. When analyzing the functioning of the system under different conditions of oxygen availability, it was possible to correlate the reaction intermediates of each systems with the activity of the *Mt*LPMO9A.

Then, the evaluation of methylene blue as a possible activator of *Mt*LPMO9A was carried out. Methylene blue is already used in biotechnological applications and has many of its characteristics known. It was determined that this photosensitizer is capable of activating *Mt*LPMO9A efficiently without the presence of an external reducer. In addition, it was determined the optimal conditions for the performance of this photobiosystem that proved to be a hybrid between the ideal conditions of *Mt*LPMO9A and the photosensitizer. Emphasizing the importance of interaction between them.

In a traditional approach of action in conjunction with ascorbic acid, it was determined that methylene blue provides improvement in the system only for the first reaction times. For longer times the system is brought to saturation faster since the amount of H_2O_2 that is being formed leads to inactivation of the enzyme. Also, in a similar way to that carried out in all the systems studied throughout the present work, the analysis of the products formed under different conditions of oxygen availability allowed the inference of the reaction intermediates.

In addition, a surprising result showed that the use of an H_2O_2 scavenger at a determined ideal conditional can greatly improve enzyme activity, since it inhibits the inactivation of the enzyme.

In short, Part II of the present work allows us to better understand the mechanism of interaction of LPMOs with photosensitizers, which is summarized in the following figure were the presented scheme is based on the study of Wang *et al.*[28] which divides the monooxygenase pathway into two routes, a route that shares a reaction intermediate with the peroxygenase pathway and is based on the protonation of the proximal O (Figure 30 a'), and (Figure 30 b') an independent route that is based on the protonation of distal O. It is also

presented the photosensitizer activation pathways, known as Type I (electron donor) and Type II (energy transfer). According to the mechanisms and their intermediates, photosensitizers would have the ability to reduce LPMO via either direct electron transfer (Figure 30 a) or superoxide radical (Figure 30 b) ($O_2^{\bullet-}$)[68] in the electron donor via. Noteworthy, the photosensitizer can provide H_2O_2 that can be used in the peroxygenase pathway of LPMO (Figure 30 c).

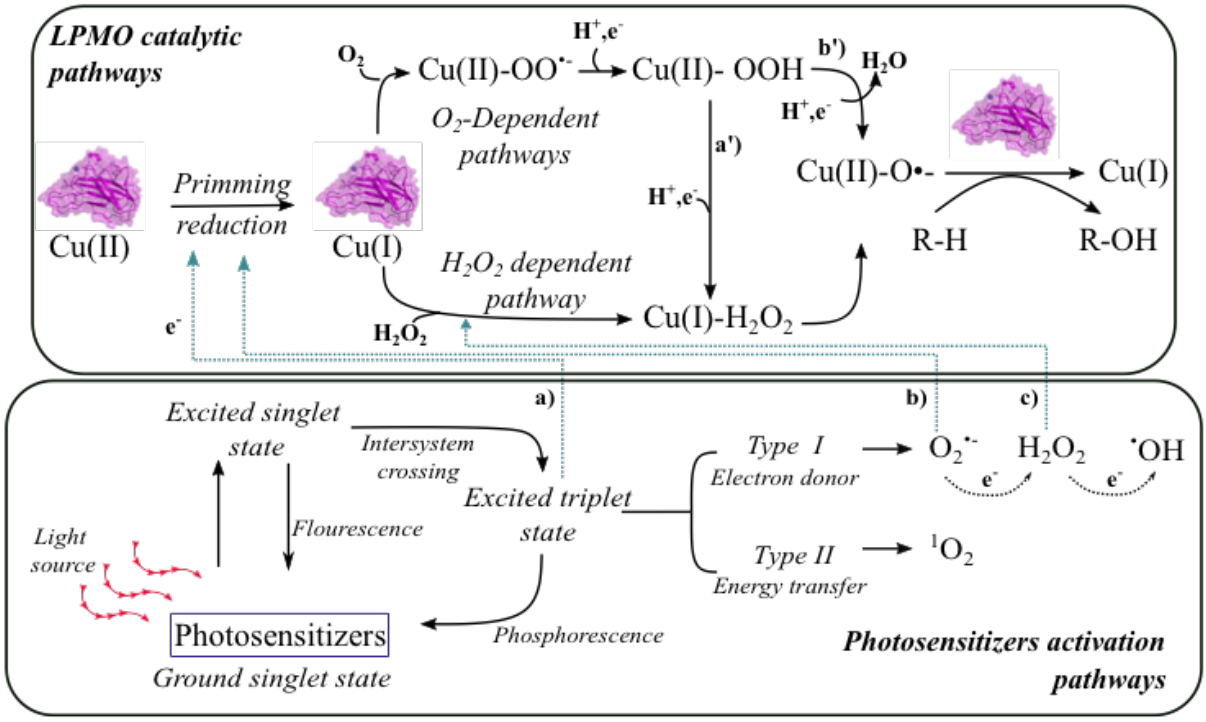

Figure 30 – General mechanism of LPMO activation by electron donor from light-activated photosensitizer. LPMO catalytic pathways for polysaccharide substrate hydroxylation can involve O_2 and H_2O_2 -dependent activities.
Source: By the author.

For this reason, the ability of a photosensitizer to activate an LPMO appears to be directly related to its ability to undergo the Type I pathway.

PART III:

General conclusions and perspectives

In the presented work, an in-depth study of the oxidative *Mt*LPMO9A can be observed. Looking at the whole panorama of the presented work, it was divided into i) characterization in terms of available knowledge, and ii) contribution to new knowledge.

In the first part, *Mt*LPMO9A was evaluated in terms of the main characteristics of LPMOs studied to date, aiming at serving as a connecting dot piece and to fill the gaps that are missing in this great puzzle of information that is still LPMOs. In this part it was possible to evaluate, from phylogeny, copper active site, going through the preference of substrate and reducing agent, use of co-substrate, and arriving in synergistic action with traditional cellulases. Thus, it was possible to cover all the theoretical aspects that affect the activity of this class of enzyme so particular as well as converging to the application aspect of depolymerization of a complex cellulosic substrate in conjunction with traditional cellulases. All the analyzes carried out demonstrated the potential of *Mt*LPMO9A as a model of high-performance LPMOs in biotechnological applications.

In the second part of the present work, it was possible to evaluate more deeply one of the branches of the study of LPMOs: the activation by light. The study started in the current state of the art with the use of chlorophyllin and, going deeper into the analysis of photosensitizers, a new activation system was developed that can be generalized once it has been identified that the good performance of a photosensitizer in a photobiosystem with LPMOs is directly related to the mechanism by which the photosensitizer performs its energy decay.

The present work, in addition to bringing the current knowledge of LPMOs, points to new areas of research and investigation mainly concerning the mechanism of activation of the enzyme and its co-substrate and the use of photosensitizers together.

Thus, the future steps are:

i) To discover which are the particular characteristics of each enzyme that make them preferentially use H_2O_2 or O_2, observing structural characteristics in more depth;

ii) Apply the light activation system with other photosensitizers also commonly used in photodynamic therapy to optimize this activation system.

REFERENCES

1 RAGAUSKAS, A. J. *et al.* The path forward for biofuels and biomaterials. **Science**, v. 311, n. 5760, p. 484–489, 2006. DOI: 10.1126/science.1114736.

2 POTHIRAJ, C.; KANMANI, P.; BALAJI, P. Bioconversion of lignocellulose materials. **Mycobiology**, v. 34, n. 4, p. 159, 2006. DOI: 10.4489/MYCO.2006.34.4.159.

3 HIMMEL, M. E. *et al.* Biomass recalcitrance: engineering plants and enzymes for biofuels production. **Science**, v. 315, n.5813, p. 804–807, 2007. DOI: 10.1126/science.1137016.

4 STEEN, E. J. *et al.* Microbial production of fatty-acid-derived fuels and chemicals from plant biomass. **Nature**, v. 463, n. 7280, p. 559–562, 2010. DOI: 10.1038/nature08721.

5 HORN, S. *et al.* Novel enzymes for the degradation of cellulose. **Biotechnology for Biofuels**, v. 5, n. 1, p. 45, 2012. DOI: 10.1186/1754-6834-5-45

6 MÜLLER, G. *et al.* Harnessing the potential of LPMO-containing cellulase cocktails poses new demands on processing conditions. **Biotechnology for Biofuels**, v. 8, n. 1, p. 187, 2015. DOI: 10.1186/s13068-015-0376-y.

7 HARRIS, P. V. *et al.* Stimulation of lignocellulosic biomass hydrolysis by proteins of glycoside hydrolase family 61: Structure and function of a large, enigmatic family. **Biochemistry**, v. 49, n. 15, p. 3305–3316, 2010. DOI: 10.1021/bi100009p.

8 ERIKSSON, K.; PETTERSSON, B.; WESTERMARK, U. Oxidation: an important enzyme reaction in fungal degradation of cellulose. **FEBS Letters**, v. 49, n. 2, p. 282–285, 1974.

9 REESE, E. T.; SIU, R. G.; LEVINSON, H. S. The biological degradation of soluble cellulose derivatives and its relationship to the mechanism of cellulose hydrolysis. **Journal of Bacteriology**, v. 59, n. 4, p. 485–497, 1950. DOI: 10.1128/jb.59.4.485- 497.1950.

10 VAAJE-KOLSTAD, G. *et al.* The non-catalytic chitin-binding protein CBP21 from Serratia marcescens is essential for chitin degradation. **Journal of Biological Chemistry**, v. 280, n. 31, p. 28492–28497, 2005. DOI:10.1074/jbc.M504468200.

11 VAAJE-KOLSTAD, G. *et al.* An oxidative enzyme boosting the enzymatic conversion of recalcitrant polysaccharides. **Science**, v. 330, n. 6001, p. 219–222, 2010. DOI:10.1126/science.1192231.

12 FORSBERG, Z. *et al.* Cleavage of cellulose by a CBM33 protein. **Protein Science**, v. 20, n. 9, p. 1479–1483, 2011. DOI:10.1002/pro.689.

13 PHILLIPS, C. M. *et al.* Cellobiose dehydrogenase and a copper-dependent polysaccharide monooxygenase potentiate cellulose degradation by Neurospora crassa. **ACS Chemical Biology**, v. 6, n. 12, p. 1399–1406, 2011. DOI:10.1021/cb200351.

14 QUINLAN, R. J. *et al.* Insights into the oxidative degradation of cellulose by a copper metalloenzyme that exploits biomass components. **Proceedings of the National Academy of Sciences**, v. 108, n. 37, p. 15079–15084, 2011. DOI: 10.1073/pnas.1105776108.

15 WESTERENG, B. *et al.* The putative endoglucanase *Pc*GH61D from *Phanerochaete chrysosporium* is a metal-dependent oxidative enzyme that cleaves cellulose. **PLoS ONE**, v. 6, n. 11, p. e27807, 2011. DOI: 10.1371/journal.pone.0027807.

16 LANGSTON, J. A. *et al.* Oxidoreductive cellulose depolymerization by the enzymes cellobiose dehydrogenase and glycoside hydrolase 61. **Applied and Environmental Microbiology**, v. 77, n. 19, p. 7007–7015, 2011. DOI: 10.1128/AEM.05815-11.

17 LEVASSEUR, A. *et al.* Expansion of the enzymatic repertoire of the CAZy database to integrate auxiliary redox enzymes. **Biotechnology for Biofuels**, v. 6, n. 1, p. 41, 2013. DOI: 10.1186/1754-6834-6-41.

18 COUTINHO, P. M. *et al.* The carbohydrate-active enzymes database (CAZy) in 2013. **Nucleic Acids Research**, v. 42, n. D1, p. D490–D495, 2013. DOI: 10.1093/nar/gkt1178.

19 CHYLENSKI, P. *et al.* Lytic Polysaccharide Monooxygenases in Enzymatic Processing of Lignocellulosic Biomass. **ACS Catalysis**, v. 9, n. 6, p. 4970–4991, 2019. DOI: 10.1021/acscatal.9b00246.

20 ZHOU, X.; ZHU, H. Current understanding of substrate specificity and regioselectivity of LPMOs. **Bioresources and Bioprocessing**, v. 7, n. 1, p. 11, 2020. DOI: 10.1186/s40643-020-0300-6.

21 FORSBERG, Z. *et al.* Polysaccharide degradation by lytic polysaccharide monooxygenases. **Current Opinion in Structural Biology**, v. 59, p. 54–64, 2019. DOI: 10.1016/j.sbi.2019.02.015.

22 KUMAR, S. *et al.* MEGA X: molecular evolutionary genetics analysis across computing platforms. **Molecular Biology and Evolution**, v. 35, n. 6, p. 1547–1549, 2018. DOI: 10.1093/molbev/msy096.

23 SAITOU, N.; NEI, M. The neighbor-joining method: a new method for reconstructing phylogenetic trees. **Molecular Biology and Evolution**, v. 4, n. 4, p. 406–25, 1987. DOI: 10.1093/oxfordjournals.molbev.a040454.

24 HEMSWORTH, G. R. *et al.* Lytic polysaccharide monooxygenases in biomass conversion. **Trends in Biotechnology**, v. 33, n. 12, p. 747–761, 2015. DOI:10.1016/j.tibtech.2015.09.006.

25 WALTON, P. H.; DAVIES, G. J. On the catalytic mechanisms of lytic polysaccharide monooxygenases. **Current Opinion in Chemical Biology**, v. 31, p. 195–207, 2016. DOI: 10.1016/j.cbpa.2016.04.001.

26 BISSARO, B. *et al.* Oxidative cleavage of polysaccharides by monocopper enzymes depends on H_2O_2. **Nature Chemical Biology**, v. 13, n. 10, p. 1123–1128, 2017. DOI: 10.1038/nchembio.2470.

27 WANG, B.; WALTON, P. H.; ROVIRA, C. Molecular mechanisms of oxygen activation and hydrogen peroxide formation in lytic polysaccharide monooxygenases. **ACS Catalysis**, v. 9, n. 6, p. 4958–4969, 2019. DOI: 10.1021/acscatal.9b00778.

28 WANG, B. *et al.* Activation of O_2 and H_2O_2 by lytic polysaccharide monooxygenases. **ACS Catalysis**, v. 10, n. 21, p. 12760–12769, 2020. DOI: 10.1021/acscatal.0c02914.

29 FRANDSEN, K. E. H.; LO LEGGIO, L. Lytic polysaccharide monooxygenases: a crystallographer's view on a new class of biomass-degrading enzymes. **IUCrJ**, v. 3, p. 448–467, 2016. DOI: 10.1107/S2052252516014147.

30 TANDRUP, T. *et al.* Recent insights into lytic polysaccharide monooxygenases (LPMOs). **Biochemical Society Transactions**, v. 46, n. 6, p. 1431–1447, 2018. DOI: 10.1042/BST20170549.

31 LI, X. *et al.* Structural basis for substrate targeting and catalysis by fungal polysaccharide monooxygenases. **Structure**, v. 20, n. 6, p. 1051–1061, 2012c. DOI: 10.1016/j.str.2012.04.002.

32 LENFANT, N. *et al.* A bioinformatics analysis of 3400 lytic polysaccharide oxidases from family AA9. **Carbohydrate Research**, v. 448, p. 166–174, 2017. DOI: 10.1016/j.carres.2017.04.012.

33 FRANDSEN, K. E. H. *et al.* Insights into an unusual auxiliary activity 9 family member lacking the histidine brace motif of lytic polysaccharide monooxygenases. **Journal of Biological Chemistry**, v. 294, n. 45, p. 17117–17130, 2019. DOI: 10.1074/jbc.RA119.009223.

34 JAGADEESWARAN, G.; VEALE, L.; MORT, A. J. Do lytic polysaccharide monooxygenases aid in plant pathogenesis and herbivory? **Trends in Plant Science**, v. 26, n. 2, p. 142–155, 2021. DOI: 10.1016/j.tplants.2020.09.013.

35 KRACHER, D. *et al*. Extracellular electron transfer systems fuel cellulose oxidative degradation. **Science**, v. 352, n. 6289, p. 1098–1101, 2016. DOI: 10.1126/science.aaf3165.

36 VOSHOL, G. P.; PUNT, P. J.; VIJGENBOOM, E. Profile comparer extended: phylogeny of lytic polysaccharide monooxygenase families using profile hidden Markov model alignments. **F1000Research**, v. 8, p. 1834, 2019. DOI: 10.12688/f1000research.21104.1.

37 SABBADIN, F. *et al.* An ancient family of lytic polysaccharide monooxygenases with roles in arthropod development and biomass digestion. **Nature Communications**, v. 9, n. 1, 2018. DOI: 10.1038/s41467-018-03142-x.

38 VOSHOL, G. P.; VIJGENBOOM, E.; PUNT, P. J. The discovery of novel LPMO families with a new Hidden Markov model. **BMC Research Notes**, v. 10, n. 1, p. 105, 2017. DOI: 10.1186/s13104-017-2429-8.

39 FREDERIKSEN, R. F. *et al*. Bacterial chitinases and chitin-binding proteins as virulence factors. **Microbiology**, v. 159, n. Pt_5, p. 833–847, 2013. DOI: 10.1099/mic.0.051839-0.

40 MEHMOOD, M. A. *et al*. Biomass production for bioenergy using marginal lands. **Sustainable Production and Consumption**, v. 9, n. July 2016, p. 3–21, 2017. DOI: 10.1016/j.spc.2016.08.003.

41 HIMMEL, M. E. *et al*. Biomass recalcitrance: engineering plants and enzymes for biofuels production. **Science**, v. 315, n. 5813, p. 804–807, 2007. DOI: 10.1126/science.1137016.

42 SCHELLER, H. V.; ULVSKOV, P. Hemicelluloses. **Annual Review of Plant Biology**, v. 61, n. 1, p. 263–289, 2010. DOI: 10.1146/annurev-arplant-042809-112315.

43 PELLEGRINI, V. O. A.; SEPULCHRO, A. G. V.; POLIKARPOV, I. Enzymes for lignocellulosic biomass polysaccharide valorization and production of nanomaterials. **Current Opinion in Green and Sustainable Chemistry**, v. 26, p. 100397, 2020. DOI: 10.1016/j.cogsc.2020.100397.

44 HARRIS, P. V. *et al.* New enzyme insights drive advances in commercial ethanol production. **Current Opinion in Chemical Biology**, v. 19, n. 1, p. 162–170, 2014. DOI: 10.1016/j.cbpa.2014.02.015.

45 MARCHLER-BAUER, A. *et al.* CDD: a conserved domain database for the functional annotation of proteins. **Nucleic Acids Research**, v. 39, n. Database, p. D225–D229, 2011. DOI: 10.1093/nar/gkq1189.

46 DYRLØV BENDTSEN, J. *et al.* Improved prediction of signal peptides: signalp 3.0. **Journal of Molecular Biology**, v. 340, n. 4, p. 783–795, 2004. DOI: 10.1016/j.jmb.2004.05.028.

47 STEENTOFT, C. *et al.* Precision mapping of the human O-GalNAc glycoproteome through SimpleCell technology. **EMBO Journal**, v. 32, n. 10, p. 1478–1488, 2013. DOI: 10.1038/emboj.2013.79.

48 LARKIN, M. A. *et al.* Clustal W and clustal X version 2.0. **Bioinformatics**, v. 23, n. 21, p. 2947–2948, 2007. DOI: 10.1093/bioinformatics/btm404.

49 BIASINI, M. *et al.* SWISS-MODEL: modelling protein tertiary and quaternary structure using evolutionary information. **Nucleic Acids Research**, v. 42, n. W1, p. W252–W258, 2014. DOI:10.1093/nar/gku340.

50 COLOVOS, C.; YEATES, T. O. Verification of protein structures: patterns of nonbonded atomic interactions. **Protein Science**, v. 2, n. 9, p. 1511–1519, 1993. DOI: 10.1002/pro.5560020916.

51 GIBSON, D. G. *et al.* Enzymatic assembly of DNA molecules up to several hundred kilobases. **Nature Methods**, v. 6, n. 5, p. 343–345, 2009. DOI: 10.1038/nmeth.1318.

52 VELASCO, J. *et al.* Heterologous expression and functional characterization of a GH10 endoxylanase from *Aspergillus fumigatus var. niveus* with potential biotechnological application. **Biotechnology Reports**, v. 24, p. e00382, 2019. DOI: 10.1016/j.btre.2019.e00382.

53 CAMILO, C. M.; POLIKARPOV, I. High-throughput cloning, expression and purification of glycoside hydrolases using Ligation-Independent Cloning (LIC). **Protein Expression and Purification**, v. 99, p. 35–42, 2014. DOI: 10.1016/j.pep.2014.03.008.

54 SEGATO, F. *et al.* High-yield secretion of multiple client proteins in *Aspergillus*. **Enzyme and Microbial Technology**, v. 51, n. 2, p. 100–106, 2012. DOI: 10.1016/j.enzmictec.2012.04.008.

55 PELLEGRINI, V. O. A. *et al.* Recombinant *Trichoderma harzianum* endoglucanase I (Cel7B) is a highly acidic and promiscuous carbohydrate-active enzyme. **Applied Microbiology and Biotechnology**, v. 99, n. 22, p. 9591–9604, 2015. DOI: 10.1007/s00253-015-6772-1.

56 PELLEGRINI, V. O. A. *et al*. Cellulose fiber size defines efficiency of enzymatic hydrolysis and impacts degree of synergy between endo- and exoglucanases. **Cellulose**, v. 25, n. 3, p. 1865–1881, 2018. DOI: 10.1007/s10570-018-1700-z.

57 KELLER, M. B. *et al.* A simple enzymatic assay for the quantification of C1-specific cellulose oxidation by lytic polysaccharide monooxygenases. **Biotechnology Letters**, v. 42, n. 1, p. 93–102, 2020a. DOI: 10.1007/s10529-019-02760-9.

58 WOOD, T. M. Preparation of crystalline, amorphous, and dyed cellulase substrates. **Methods in Enzymology**, v. 160, p. 19–25, 1988. DOI: 10.1016/0076-6879(88)60103-0.

59 KITTL, R. *et al.* Production of four *Neurospora crassa* lytic polysaccharide monooxygenases in *Pichia pastoris* monitored by a fluorimetric assay. **Biotechnology for Biofuels**, v. 5, n. 1, p. 79, 2012. DOI: 10.1186/1754-6834-5-79.

60 MILLER, G. L. Use of dinitrosalicylic acid reagent for determination of reducing sugar. **Analytical Chemistry**, v. 31, n. 3, p. 426–428, 1959. DOI: 10.1021/ac60147a030.

61 FROMMHAGEN, M. *et al.* Lytic polysaccharide monooxygenases from *Myceliophthora thermophila* C1 differ in substrate preference and reducing agent specificity. **Biotechnology for Biofuels**, v. 9, n. 1, p. 186, 2016. DOI: 10.1186/s13068-016-0594-y.

62 FROMMHAGEN, M. *et al.* Discovery of the combined oxidative cleavage of plant xylan and cellulose by a new fungal polysaccharide monooxygenase. **Biotechnology for Biofuels**, v. 8, n. 1, p. 101, 2015. DOI: 10.1186/s13068-015-0284-1.

63 BEESON, W. T. *et al.* Oxidative cleavage of cellulose by fungal copper-dependent polysaccharide monooxygenases. **Journal of the American Chemical Society**, v. 134, n. 2, p. 890–892, 2012. DOI: 10.1021/ja210657t.

64 VU, V. V. *et al.* Determinants of regioselective hydroxylation in the fungal polysaccharide monooxygenases. **Journal of the American Chemical Society**, v. 136, n. 2, p. 562–565, 2014. DOI: 10.1021/ja409384b.

65 ISAKSEN, T. *et al.* A C4-oxidizing lytic polysaccharide monooxygenase cleaving both cellulose and cello-oligosaccharides. **Journal of Biological Chemistry**, v. 289, n. 5, p. 2632–2642, 2014. DOI: 10.1074/jbc.M113.530196.

66 VELASCO, J. *et al.* Comparative analysis of two recombinant LPMOs from *Aspergillus fumigatus* and their effects on sugarcane bagasse saccharification. **Enzyme and Microbial Technology**, v. 144, p. 109746, 2021. DOI: 10.1016/j.enzmictec.2021.109746.

67 STEPNOV, A. A. *et al.* Unraveling the roles of the reductant and free copper ions in LPMO kinetics. **Biotechnology for Biofuels**, v. 14, n. 1, p. 28, 2021. DOI: 10.1186/s13068-021-01879-0.

68 BISSARO, B. *et al.* Controlled depolymerization of cellulose by light-driven lytic polysaccharide oxygenases. **Nature Communications**, v. 11, n. 1, p. 890, 2020. DOI: 10.1038/s41467-020-14744-9.

69 SONG, B. *et al.* Real-time imaging reveals that lytic polysaccharide monooxygenase promotes cellulase activity by increasing cellulose accessibility. **Biotechnology for Biofuels**, v. 11, n. 1, p. 41, 2018. DOI: 10.1186/s13068-018-1023-1.

70 EIBINGER, M. *et al.* Single-molecule study of oxidative enzymatic deconstruction of cellulose. **Nature Communications**, v. 8, n. 1, p. 894, 2017. DOI: 10.1038/s41467-017-01028-y.

71 VERMAAS, J. V. *et al.* Effects of lytic polysaccharide monooxygenase oxidation on cellulose structure and binding of oxidized cellulose oligomers to cellulases. **Journal of Physical Chemistry B**, v. 119, n. 20, p. 6129–6143, 2015. DOI: 10.1021/acs.jpcb.5b00778.

72 ZHOU, H. *et al.* A lytic polysaccharide monooxygenase from *Myceliophthora thermophila* and its synergism with cellobiohydrolases in cellulose hydrolysis. **International Journal of Biological Macromolecules**, v. 139, p. 570–576, 2019. DOI: 10.1016/j.ijbiomac.2019.08.004.

73 KELLER, M. B. *et al.* Promoting and impeding effects of lytic polysaccharide monooxygenases on glycoside hydrolase activity. **ACS Sustainable Chemistry & Engineering**, v. 8, n. 37, p. 14117–14126, 2020b. DOI:10.1021/acssuschemeng.0c04779.

74 EIBINGER, M. *et al.* Cellulose surface degradation by a lytic polysaccharide monooxygenase and its effect on cellulase hydrolytic efficiency. **Journal of Biological Chemistry**, v. 289, n. 52, p. 35929–35938, 2014. DOI: 10.1074/jbc.M114.602227.

75 KIRK, O.; BORCHERT, T. V.; FUGLSANG, C. C. Industrial enzyme applications. **Current Opinion in Biotechnology**, v. 13, n. 4, p. 345–351, 2002. DOI: 10.1016/S0958-1669(02)00328-2.

76 LI, S. *et al.* Technology prospecting on enzymes: application, marketing and engineering. **Computational and Structural Biotechnology Journal**, v. 2, n. 3, p. e201209017, 2012b. DOI: 10.5936/csbj.201209017.

77 PAYNE, C. M. *et al.* Fungal cellulases. **Chemical Reviews**, v. 115, n. 3, p. 1308–1448, 2015. DOI: 10.1021/cr500351c.

78 BHATKHANDE, D. S.; PANGARKAR, V. G.; BEENACKERS, A. A. Photocatalytic degradation for environmental applications - a review. **Journal of Chemical Technology & Biotechnology**, v. 77, n. 1, p. 102–116, 2002. DOI: 10.1002/jctb.532.

79 DOLMANS, D. E. J. G. J.; FUKUMURA, D.; JAIN, R. K. Photodynamic therapy for cancer. **Nature Reviews Cancer**, v. 3, n. 5, p. 380–387, 2003. DOI: 10.1038/nrc1071.

80 SEEL, C. J.; GULDER, T. biocatalysis fueled by light: on the versatile combination of photocatalysis and enzymes. **ChemBioChem**, v. 20, n. 15, p. 1871–1897, 2019. DOI: 10.1002/cbic.201800806.

81 HUDLICKY, T.; REED, J. W. Applications of biotransformations and biocatalysis to complexity generation in organic synthesis. **Chemical Society Reviews**, v. 38, n. 11, p. 3117, 2009. DOI: 10.1039/b901172m.

82 SHELDON, R. A.; WOODLEY, J. M. Role of biocatalysis in sustainable chemistry. **Chemical Reviews**, v. 118, n. 2, p. 801–838, 2018. DOI: 10.1021/acs.chemrev.7b00203.

83 ARNOLD, F. H. Design by directed evolution. **Accounts of Chemical Research**, v. 31, n. 3, p. 125–131, 1998. DOI: 10.1021/ar960017f.

84 SCHMERMUND, L. *et al*. Photo-biocatalysis: biotransformations in the presence of light. **ACS Catalysis**, v. 9, n. 5, p. 4115–4144, 2019. DOI: 10.1021/acscatal.9b00656.

85 MICHELIN, C.; HOFFMANN, N. Photosensitization and photocatalysis - perspectives in organic synthesis. **ACS Catalysis**, v. 8, n. 12, p. 12046–12055, 2018. DOI: 10.1021/acscatal.8b03050.

86 RAVELLI, D. *et al.* Photocatalysis. a multi-faceted concept for green chemistry. **Chemical Society Reviews**, v. 38, n. 7, p. 1999, 2009. DOI: 10.1039/b714786b.

87 MARZO, L. *et al*. Visible-light photocatalysis: does it make a difference in organic synthesis? **Angewandte Chemie International Edition**, v. 57, n. 32, p. 10034–10072, 2018. DOI: 10.1002/anie.201709766.

88 CANNELLA, D. *et al*. Light-driven oxidation of polysaccharides by photosynthetic pigments and a metalloenzyme. **Nature Communications**, v. 7, n. 1, p. 11134, 2016. DOI: 10.1038/ncomms11134.

89 BISSARO, B. *et al.* Fueling biomass-degrading oxidative enzymes by light-driven water oxidation. **Green Chemistry**, v. 18, n. 19, p. 5357–5366, 2016. DOI: 10.1039/C6GC01666A.

90 BLOSSOM, B. M. *et al.* Photobiocatalysis by a lytic polysaccharide monooxygenase using intermittent illumination. **ACS Sustainable Chemistry & Engineering**, v. 8, n. 25, p. 9301–9310, 2020. DOI: 10.1021/acssuschemeng.0c00702.

91 DETTY, M. R.; GIBSON, S. L.; WAGNER, S. J. Current clinical and preclinical photosensitizers for use in photodynamic therapy. **Journal of Medicinal Chemistry**, v. 47, n. 16, p. 3897–3915, 2004. DOI: 10.1021/jm040074b.

92 PERNAMBUCO, U. *et al.* Photodynamic effects of curcumin in biofilms and carious dentine photodynamic antimicrobial therapy of curcumin in biofilms and carious dentine. **Lasers in Medical Science**, v.29, n.2, p. 629-635, 2014. DOI: 10.1007/s10103-013-1369-3.

93 ANDRADE, M. C. *et al.* Effect of different pre-irradiation times on curcumin-mediated photodynamic therapy against planktonic cultures and biofilms of Candida spp. **Archives of Oral Biology**, v. 58, n. 2, p. 200–210, 2013. DOI: 10.1016/j.archoralbio.2012.10.011.

94 OCHSNER, M. Photophysical and photobiological processes in the photodynamic therapy of tumours. **Journal of Photochemistry and Photobiology B:** biology, v. 39, n. 1, p. 1–18, 1997.DOI: 10.1016/S1011-1344(96)07428-3.

95 LIU, Y. *et al.* Antibacterial photodynamic therapy: overview of a promising approach to fight antibiotic-resistant bacterial infections. **Journal of Clinical and Translational Research**, 2015. DOI: 10.18053/jctres.201503.002.

96 JUNQUEIRA, H. C. *et al.* Modulation of methylene blue photochemical properties based on adsorption at aqueous micelle interfaces. **Physical Chemistry Chemical Physics**, v. 4, n. 11, p. 2320–2328, 2002. DOI: 10.1039/b109753a.

97 CHEN, J.; CESARIO, T. C.; RENTZEPIS, P. M. Effect of pH on methylene blue transient states and kinetics and bacteria photoinactivation. **Journal of Physical Chemistry A**, v. 115, n. 13, p. 2702–2707, 2011. DOI: 10.1021/jp110215g.

98 ABELE, D. *et al.* Temperature-dependence of mitochondrial function and production of reactive oxygen species in the intertidal mud clam Mya arenaria. **Journal of Experimental Biology**, v. 205, n. Pt 13, p. 1831–1841, 2002. DOI: http://www.ncbi.nlm.nih.gov/pubmed/12077159.

99 AGGER, J. W. *et al.* Discovery of LPMO activity on hemicelluloses shows the importance of oxidative processes in plant cell wall degradation. **Proceedings of the National Academy of Sciences**, v. 111, n. 17, p. 6287–6292, 2014. DOI: 10.1073/pnas.1323629111.

100 KADOWAKI, M. A. S. *et al.* Functional characterization of a lytic polysaccharide monooxygenase from the thermophilic fungus *Myceliophthora thermophila*. **PLoS ONE**, v. 13, n. 8, p. e0202148, 2018. DOI: 10.1371/journal.pone.0202148.

101 HOFFMANN, M. R.; EDWARDS, J. O. Kinetics of the oxidation of sulfite by hydrogen peroxide in acidic solution. **Journal of Physical Chemistry**, v. 79, n. 20, p. 2096–2098, 1975. DOI: 10.1021/j100587a005.

102 LI, R. *et al.* Enhancing effect of alcoholic solvent on hydrosulfite–hydrogen peroxide chemiluminescence system. **Journal of Physical Chemistry A**, v. 116, n. 9, p. 2192–2197, 2012a. DOI: 10.1021/jp300012t.

103 BRAWLEY, V.; BHATIA, J.; KARP, W. B. Effect of sodium metabisulfite on hydrogen peroxide production in light-exposed pediatric parenteral amino acid solutions. **American Journal of Health-System Pharmacy**, v. 55, n. 12, p. 1288–1292, 1998. DOI: 10.1093/ajhp/55.12.1288.

Annex

Publications related to the master's period:

Published articles:

- SEPULCHRO, A. G. V. *et al.* Magnetoreception in multicellular magnetotactic prokaryotes: a new analysis of escape motility trajectories in different magnetic fields. **European Biophysics Journal**, v. 49, n. 7, p. 609–617, 8 out. 2020.
- SEPULCHRO, A. G. V. *et al.* Transformation of xylan into value-added biocommodities using Thermobacillus composti GH10 xylanase. **Carbohydrate Polymers**, v. 247, n. May, p. 116714, nov. 2020.
- PELLEGRINI, V. DE O. A.; SEPULCHRO, A. G. V.; POLIKARPOV, I. Enzymes for lignocellulosic biomass polysaccharide valorization and production of nanomaterials. **Current Opinion in Green and Sustainable Chemistry**, v. 26, p. 100397, dez. 2020.
- VACILOTTO, M. M. *et al.* Production of prebiotic xylooligosaccharides from arabino- and glucuronoxylan using a two-domain Jonesia denitrificans xylanase from GH10 family. **Enzyme and Microbial Technology**, v. 144, p. 109743, mar. 2021.
- VELASCO, J. *et al.* Comparative analysis of two recombinant LPMOs from Aspergillus fumigatus and their effects on sugarcane bagasse saccharification. **Enzyme and Microbial Technology**, p. 109746, jan. 2021.

Submitted article:

- SEPULCHRO, A. G. V. *et al.* Chlorophyllin-mediated light activation and co-substrate preferences of lytic polysaccharide monooxygenase *Mt*LPMO9A - This work is under review on Biofuel Research Journal under protocol: BRJ-2105-2111

Article in preparation:

- SEPULCHRO, A. G. V. *et al.* Methylene blue: a photosensitizer capable of efficient light induced activation of lytic polysaccharide monooxygenases - This work is written and is being corrected by the supervisor.

Academic award in the master's period:

Yvonne Mascarenhas Award for Best Master's degree Research for the study: "The lytic polysaccharide monooxygenase from *Myceliophthora thermophila* (*Mt*LPMO9A) as a model for high-efficiency LPMOs in biotechnological processes"; presented in virtual poster and oral presentation. 10ª Integrated Week of São Carlos Institute of Physics, University of São Paulo – 2020.